




Simultaneous administration of cocaine and caffeine dysregulates HCN and T-type channels

María Celeste Rivero-Echeto¹ · Paula P. Perissinotti¹ · Carlota González-Inchauspe¹ · Lucila Kargieman¹ · Verónica Bisagno² · Francisco J. Urbano^{1,3,4} 

Received: 6 October 2020 / Accepted: 18 November 2020 / Published online: 25 November 2020
© Springer-Verlag GmbH Germany, part of Springer Nature 2020

Abstract

Rationale The abuse of psychostimulants has adverse consequences on the physiology of the central nervous system. In Argentina, and other South American countries, coca paste or “PACO” (cocaine and caffeine are its major components) is massively consumed with deleterious clinical consequences for the health and well-being of the general population. A scant number of studies have addressed the consequences of stimulant combination of cocaine and caffeine on the physiology of the somatosensory thalamocortical (ThCo) system.

Objectives Our aim was to study ion conductances that have important implications regulating sleep–wake states 24-h after an acute or chronic binge-like administration of a cocaine and caffeine mixture following previously analyzed pasta base samples (“PACO”-like binge”) using mice.

Methods We randomly injected (i.p.) male C57BL/6JFcen mice with a binge-like psychostimulants regimen during either 1 day (acute) or 1 day on/1 day off during 13 days for a total of 7 binges (chronic). Single-cell patch-clamp recordings of VB neurons were performed in thalamocortical slices 24 h after the last psychostimulant injection. We also recorded EEG/EMG from mice 24 h after being systemically treated with chronic administration of cocaine + caffeine versus saline, vehicle.

Results Our results showed notorious changes in the intrinsic properties of the VB nucleus neurons that persist after 24-h of either acute or chronic binge administrations of combined cocaine and caffeine (“PACO”-like binge). Functional dysregulation of HCN (hyperpolarization-activated cyclic nucleotide-gated) and T-type VGC (voltage-gated calcium) channels was described 24-h after acute/chronic “PACO”-like administrations. Furthermore, intracellular basal $[Ca^{2+}]$ disturbances resulted a key factor that modulated the availability and the activation of T-type channels, altering T-type “window currents.” As a result, all these changes ultimately shaped the low-threshold spikes (LTS)-associated Ca^{2+} transients, regulated the membrane excitability, and altered sleep–wake transitions.

Conclusion Our results suggest that deleterious consequences of stimulants cocaine and caffeine combination on the thalamocortical physiology as a whole might be related to potential neurotoxic effects of soaring intracellular $[Ca^{2+}]$.

María Celeste Rivero-Echeto and Paula P. Perissinotti contributed equally to this work.

Carlota González-Inchauspe In memoriam (1968–June 2020)

✉ Francisco J. Urbano
fjurbano@fbmc.fcen.uba.ar

María Celeste Rivero-Echeto
macesteriveroechoeto@gmail.com

Paula P. Perissinotti
peripali@fbmc.fcen.uba.ar

Lucila Kargieman
lukargieman@fbmc.fcen.uba.ar

Verónica Bisagno
vbisagno@ffy.uba.ar

¹ CONICET-Universidad de Buenos Aires, Instituto de Fisiología, Biología Molecular y Neurociencias (IFIBYNE), Ciudad de Buenos Aires, Argentina

² CONICET-Universidad de Buenos Aires, Instituto de Investigaciones Farmacológicas (ININFA), Ciudad de Buenos Aires, Argentina

³ Universidad de Buenos Aires, Facultad de Ciencias Exactas y Naturales, Departamento de Fisiología, Biología Molecular y Celular “Dr. Héctor Maldonado”, Ciudad de Buenos Aires, Argentina

⁴ IFIBYNE (UBA-CONICET), Intendente Güiraldes 2160, Ciudad Universitaria, C1428EGA Ciudad Autónoma de Buenos Aires, Argentina

Keywords Cocaine · Caffeine · Thalamic ventrobasal · Calcium imaging · HCN channels · T-type channels · Mouse

Abbreviations

ACSF	Artificial cerebrospinal fluid
APs	Action potentials
CNQX	6-Cyano-7-nitroquinoxaline-2,3-dione disodium salt hydrate
HCN	Hyperpolarization-activated cyclic nucleotide-gated
VGC	Voltage-gated calcium
DL-AP5	DL-2-amino-5-phosphonovaleric acid
EGTA	Ethylene glycol-bis (β -aminoethyl ether)-N,N,N',N'-tetraacetic acid tetrasodium salt
LTS	Low-threshold voltage-gated T-type-mediated spike
TEA	Tetraethylammonium
ThCo	Thalamocortical
TTX	Tetrodotoxin
VB	Ventrobasal

Introduction

The abuse of psychostimulants represents a health problem and includes adverse consequences on the physiology of the central nervous system. Cannabinoids, opiates, cocaine, amphetamine, methamphetamine, and “ecstasy” stand out among the most commonly abused drugs (Cadet and Bisagno 2013; Cadet et al. 2014), which are combined with newly designed drugs (bath salts) whose deleterious effects are still far from being fully known (López-Rodríguez and Viveros 2019). In South America and especially in Argentina, the Oriental Republic of Uruguay and other South American countries, coca “paste” or “PACO” (which represents another inhalable form of cocaine besides crack) is massively consumed (Prieto et al. 2016; Schwarzkopf et al. 2018).

López-Hill et al. (2011) have described the most common components of the cocaine base “paste” samples seized by the Uruguayan police, showing that the percentage of cocaine varies between 20 and 50%, while there is an alarmingly high percentage of caffeine that reaches between 20% and 30% (López-Hill et al. 2011). Caffeine used as an adulterant, volatile when smoked, would work in synergy with cocaine to increase the stimulating effect and its consumption is associated with a very high abuse liability and toxicity (Prieto et al. 2016, 2020). In mice, systemic chronic administration of a combination of cocaine and caffeine that emulated the proportion described on pasta base samples (López-Hill et al. 2011) induced an initial increase in motor activity (Muñiz et al. 2016) and altered

the expression of genes involved in glutamatergic and dopaminergic neurotransmission in the mesolimbic reward system (Muñiz et al. 2017). Caffeine effects on thalamocortical (ThCo) neurons have been described to involve altered calcium release and reuptake by the endoplasmic reticulum (Coulon et al. 2009; Rankovic et al. 2010), while inhibiting phosphodiesterase (Fontanez and Porter 2006; Rankovic et al. 2010) and blocking adenosine receptors that play a central role on wake-sleep cycles (Lazarus et al. 2011). Indeed, caffeine enhanced wakefulness-induced effects of cocaine in rodents when using coca “paste” samples during electroencephalographic recordings (Schwarzkopf et al. 2018).

Cocaine alters somatosensory ThCo processing through the increment of monoamine synaptic levels (Urbano et al. 2015; Bisagno et al. 2016; Urbano and Bisagno 2017). Excessive cocaine use can cause manifestations extensively related to alter ThCo processing (Behrendt 2006) like seizures and delusions accompanied by hallucinations (Hanson et al. 1999; Devlin and Henry 2008).

A scant number of studies have addressed the consequences of stimulants combination of cocaine and caffeine on the physiology of the somatosensory ThCo system. In this study, mice were injected with a mixture of cocaine and caffeine (PACO-like binge), whose composition resembles previously analyzed “cocaine paste base” samples (López-Hill et al. 2011). We focused on the study of how PACO-like administrations alter ion conductances that have important implications regulating sleep–wake states. In particular, I_H (the current mediated by hyperpolarization-activated cyclic nucleotide-gated channels, i.e., HCN channels) and I_T (T-type calcium current mediated by Ca_v3 channels) are key conductances known to modulate neuronal activity within the subthreshold voltage range (Jahnsen and Llinás 1984a, b; Urbano and Bisagno 2017; Zobeiri et al. 2018, 2019). Firstly, we characterized I_H and I_T activity in mice ThCo ventrobasal (VB) neurons 24-h after an acute administration of a “PACO”-like binge. Then, we assessed whether the acute alterations that we found persisted or changed 24-h after a chronic administration; studying also sleep–wake transitions during electroencephalography sleep recordings. We found a functional dysregulation of HCN and T-type channels 24-h after acute/chronic “PACO”-like administrations. In addition, intracellular basal $[Ca^{2+}]$ alterations modulated the availability and the activation of T-type channels, affecting T-type “window currents.” As a result, all these changes ultimately shaped LTS-associated Ca^{2+} transients, regulated the membrane excitability, and altered sleep–wake transitions.

Materials and methods

Animals

We used male C57BL/6JF₁ mice (25–35 days old, 25–30 g). Central Animal Facility at the University of Buenos Aires, animal protocol #50–2015, and #67–2015). Principles of animal care were in accordance with the ARRIVE guidelines and CONICET (2003), and approved by its authorities using OLAW/ARENA directives (NIH, Bethesda, MD, USA). Mice were monitored regularly by researchers in charge of handling and injections. No exclusion criteria were pre-determined. None of the mice died from treatment or injection procedure. We minimized suffering by carefully injecting the mice, placing the injected animals in a warm and comfortable environment in their home cage.

Researcher blindly and randomly injected mice. Researchers in charge of electrophysiological recordings, analysis of data, and statistical comparisons were blind to treatment schedules (i.e., the experimenter was unaware of the animal's group assignment). A simple randomization procedure was used to assign mice to either vehicle or psychostimulant treatment.

Psychostimulants administration

A simple randomization procedure was used to assign mice to either vehicle or psychostimulant treatments. Cocaine hydrochloride and caffeine (Sigma-Aldrich, St Louis, MO) were administered in a binge-like regimen of three i.p. injections per day, 1 h apart, following an intermittent protocol of administration, i.e., mice received binge injections during either 1 day (acute) or 1 day on/1 day off during 13 days for a total of 7 binges (chronic) (Muñiz et al. 2016, 2017). Animals were randomly assigned to four different groups: cocaine (Coc, 3 × 10 mg/kg), caffeine (Caf, 3 × 5 mg/kg), Coc + Caf (3 × Cocaine+Caffeine combined solution: Coc 10 mg/kg + Caf 5 mg/kg, both dissolved in the same sterile saline solution and co-administered in a single injection), or Veh (3 × saline).

Thalamocortical slices and whole-cell patch-clamp recordings

Slices were obtained 24 h after the last injection of either acute or chronic protocol (Urbano et al. 2009; Bisagno et al. 2010; Goitia et al. 2013, 2016; Perissinotti et al. 2018). Mice were deeply anesthetized with tribromoethanol (250 mg/kg; i.p.) followed by transcardial perfusion with ice-cold low sodium/antioxidant solution (composition in mM: 200 sucrose, 2.5 KCl, 3 MgSO₄, 26 NaHCO₃, 1.25 NaH₂PO₄, 20 D-glucose, 0.4 ascorbic acid, 2 pyruvic acid, 1 kynurenic acid, 1 CaCl₂, and aerated with 95% O₂, 5% CO₂, pH 7.4), and then decapitated. Thalamocortical brain slices (300 μm) were obtained

by gluing both hemispheres onto a vibratome stage (PELCO, EasiSlicer, Ted Pella Inc., CA, USA), submerged in a chamber containing chilled low-sodium/high-sucrose solution (composition in mM: 250 sucrose, 2.5 KCl, 3 MgSO₄, 0.1 CaCl₂, 1.25 NaH₂PO₄, 0.4 ascorbic acid, 3 myo-inositol, 2 pyruvic acid, 25 D-glucose, and 25 NaHCO₃). Slices were cut sequentially and transferred to an incubation chamber at 35 °C for 30 min containing a stimulant-free, low Ca²⁺/high Mg²⁺ normal artificial cerebrospinal fluid (ACSF) (composition in mM: 125 NaCl, 2.5 KCl, 3 MgSO₄, 0.1 CaCl₂, 1.25 NaH₂PO₄, 0.4 ascorbic acid, 3 myo-inositol, 2 pyruvic acid, 25 d-glucose, and 25 NaHCO₃ and aerated with 95% O₂/5% CO₂, pH 7.4).

Whole-cell patch-clamp recordings of ventrobasal (VB) thalamocortical neurons were performed at room temperature (20–24 °C) in normal ACSF with MgCl₂ (1 mM) and CaCl₂ (2 mM). Patch electrodes were made from borosilicate glass (2–3 MΩ) filled with either high K⁺ solution (composition in mM: 110 potassium gluconate, 30 KCl, 10 HEPES, 10 Na₂ phosphocreatine, 0.2 EGTA, 2 Mg-ATP 2, 0.5 Li-GTP, and 1 MgCl₂; pH was adjusted to 7.3 with KOH) or high Cl⁻, high Cs⁺/QX314 solution (composition in mM: 110 CsCl, 40 HEPES, 10 TEA-Cl, 12 Na₂ phosphocreatine, 0.5 EGTA, 2 Mg-ATP, 0.5 Li-GTP, and 1 MgCl₂. pH was adjusted to 7.3 with CsOH). When needed, voltage-dependent Na⁺ currents/postsynaptic action potentials were blocked using 10 mM *N*-(2,6-diethylphenyl)carbamoylmethyl triethylammonium chloride (QX-314) in the intracellular solution. Signals were recorded using a MultiClamp 700 amplifier commanded by pCLAMP 10.0 software (Molecular Devices, CA, USA). Data were filtered at 5 kHz, digitized, and stored for off-line analysis.

Cell capacitance was measured from a transient current evoked by a 5-mV depolarizing step from a holding potential of –90 mV. Cells with series resistance (R_s) < 15 MΩ were used after being compensated online (> 80%).

Hyperpolarization-activated cyclic nucleotide-gated (HCN)-mediated currents

Hyperpolarization-activated cyclic nucleotide-gated (HCN) or H-currents (I_H) were studied in “voltage-clamp” mode using a K-Gluconate intracellular solution. I_H is a nonspecific cationic current that is activated by hyperpolarization of the membrane and was pharmacologically isolated using specific blockers for voltage-gated sodium channels (TTX 3 μM), potassium channels (TEA; 10 mM, BaCl₂; 0.5 mM), calcium channels (CdCl₂; 0.1 mM), and glutamate receptors NMDA (AP-5 50 μM) and AMPA (CNQX; 20 μM), plus GABA-A receptors (Bicuculline; 50 μM). In order to identify I_H, the specific blocker for it was used ZD7288 (30 μM) (Lüthi et al. 1998; Zhang et al. 2016). Once I_H current was identified, a protocol was implemented in order to increase the stability of the

registers in the “voltage-clamp” mode, as well as to account for its increasing activation speed (Kanyshkova et al. 2009). I_H steady-state activation (SSA) was estimated by normalizing the tail current amplitudes measured 50 ms after a variable prepulse holding potential (from -40 to -130 mV) to a fixed holding potential of -100 mV. The following equation was used in order to fit SSA:

$$V = (I(V) - I_{\min}) / (I_{\max} - I_{\min}),$$

where I_{\max} being the amplitude of the tail current for the voltage step from -130 to -100 mV and I_{\min} for the voltage step from -40 to -100 mV. I_H activation was fitted to the Boltzmann equation:

$$I/I_{\max} = 1 / (1 + \exp((V - V_{50})/k))$$

where V is the membrane potential of the prepulse, V_{50} is the membrane potential in which half of I_H is activated, and k is the slope or “slow factor” (Momin et al. 2008).

Biophysical parameters of T-type calcium currents and low-threshold spikes

T-type voltage-gated calcium currents (I_T) were generated in voltage-clamp using an intracellular solution based on high Cl^- , high Cs^+ /QX-314. I_T was pharmacologically isolated adding the following specific blockers to ACSF: TTX ($3 \mu M$), TEA (10 mM), DL-AP-5 ($50 \mu M$), CNQX ($20 \mu M$), Bicucullin ($50 \mu M$). Voltage dependence of I_T was studied using square pulses initially to hyperpolarizing holding potentials to de-inactivate T-type channels, followed by depolarizing holding pulses (Perissinotti et al. 2014). Hyperpolarization time and depolarizing pulses varied between experiments. T-type current conductance was calculated using an I-V protocol of depolarizing voltage holding steps from -110 to -45 mV in 5 mV steps. For each voltage step applied, the conductance $G(V_H) = I_T(V_H) / (V_H - 40$ mV) was calculated, where I_T is the current activated by the voltage holding (V_H) and 40 mV is the estimated reversal potential for calcium. To determine the voltage dependence of the fraction of channels available to be activated, a “steady-state inactivation” (SSI) protocol was used (Perissinotti et al. 2014): pre-pulse, holding potential was brought from -110 to -45 mV in 5 mV steps, during 500 ms to de-inactivate T-type channels. Test pulse, the fraction of T-type channels available were tested at a single step to a holding of -50 mV. $I_T/I_{T,\max}$ ratio was plotted as a function of holding potential (V_H).

Both activation and inactivation curves for I_T were fitted to a Boltzmann equation:

$$\text{Activation curve, } G/G_{\max} = 1 / \left(1 + \exp\left(\frac{V - V_{50}}{k}\right) \right)$$

$$\text{Inactivation curve, } I_T/I_{T,\max} = 1 / \left(1 + \exp\left(\frac{V - V_{50}}{k}\right) \right)$$

where G is the conductance for each holding potential pulse, and G_{\max} the maximum conductance. $I_T/I_{T,\max}$ is the available fraction of T channels and its dependence on voltage represents the inactivation curve. V_{50} represents the voltage at which 50% of the total population of channels was activated/inactivated, respectively; k is a slope factor indicating I_T currents voltage-dependence. We've used the following equation to calculate the theoretical “Window current” (i.e., the overlapping section after fitting to a Boltzmann equation both activation and inactivation curves):

$$I_T(\text{stst}) = G(V_H) * I_T / I_{T,\max}(V_H) * (V_H - 40 \text{ mV})$$

where $I_T(\text{stst})$ is the current in the steady-state or “window current,” G is the conductance at holding voltage V_H , $I_T / I_{T,\max}$ is the fraction of T-type channels available at holding voltage V_H , and 40 mV is the estimated reversal potential for calcium. Reversal potential for Ca^{2+} ions (E_{Ca}) was calculated using average current-voltage (I-V) curves from holding current pulses ($n = 16$) or current ramps ($n = 13$) during VB recordings.

Current-clamp experiments

Current-clamp experiments were performed using a K-Gluconate intracellular solution. No spontaneous action potential (AP) discharge was observed at resting membrane potential during whole-cell recordings of VB thalamocortical neurons.

Resting membrane potential (RMP) was recorded in continuous trace mode without current injection for 20 s, and averaged; voltages were corrected for liquid junction potentials.

Whole cell input resistance (R_{in}) was determined as the slope obtained from instantaneous voltage-current relationships (V-I curves). V-I curves were constructed using current steps progressing at 100 pA increments, starting from -500 to 100 pA (500 ms duration).

Low-threshold spikes (LTS) were generated using a hyperpolarizing current pulse of -100 or -200 pA for 500 ms.

Membrane excitability was calculated after applying an hyperpolarizing current step (-200 pA for 50 ms), AP discharges were elicited by injection of a depolarizing current ramp (from -200 to 800 pA during 1.5 s, ramp rate = 667 pA/s). The membrane potential was held at -65 mV (V_H). The action potential voltage threshold was determined using the first derivative of the first AP.

Ratiometric calcium imaging

Ca²⁺-imaging in VB neurons was performed concurrently with whole-cell recordings using an Andor iXon+ EMCCD camera (512 × 512, Andor tech., Belfast, UK) coupled to a monochromator Polychrome V (TILL Photonics GmbH, Munich, Germany) through an optic fiber connected to a BX51WI Olympus upright microscope (Olympus Latin America Inc., FL, USA). To allow sufficient intercellular filling of VB neurons with dye, imaging was initiated 5–10 min after obtaining whole-cell configuration. The ratiometric Ca²⁺-sensitive indicator fura-2 (in vitro K_d = 224 nM) allowed a more accurate report of the time course and amplitude of intracellular [Ca²⁺] dynamics at somatic and proximal dendrites level (Rozas et al. 2017). Fluorescence changes at 510 nm were acquired after consecutive 340 nm and 380 nm wavelengths using a 0.8 numerical aperture water-immersion 40× objective (Olympus Latin America Inc., FL, USA). Image acquisition was performed using cell-R software (Olympus Soft Imaging Solutions, Münster, Germany), and analyzed post hoc using NIH Image J software. Imaging protocol consisted of 50 images (130 ms exposition time) to calculate background fluorescence prior to a hyperpolarizing current pulse of –200 pA of 500 ms duration in current-clamp using a K-Gluconate intracellular solution. Then, 150 images were taken after hyperpolarizing current pulse. Fluorescence ratio (F₃₄₀/F₃₈₀) was estimated offline to intracellular Ca²⁺ concentration ([Ca²⁺]_i) using a calibration curve (Rankovic et al. 2010; Di Guilmi et al. 2014). No dye saturation was appreciated during analysis of experiments that used current injection of hyperpolarizing pulses. However, R_{max} is the highest ratio value obtained when Fura-2 is saturated following previously described protocols (Usachev et al. 1993; Rankovic et al. 2010; Di Guilmi et al. 2014). R_{min} was the minimum ratio obtained in the absence of calcium (Usachev et al. 1993; Rankovic et al. 2010; Di Guilmi et al. 2014).

Electroencephalography/electromyography recordings

Mice were deeply anesthetized on a thermal blanket (36 °C) using a gaseous mixture of isoflurane (2% in O₂) and placed in a stereotaxic frame. After exposing the skull, four electroencephalography (EEG) recording screws with attached wires (0.10" screw with wire leads, Part #8403, Pinnacle Technology, Inc., Lawrence, KS) were placed contralaterally across the somatosensory/motor cortex, ground electrode between preculminate and primary fissure, cerebellum, while electromyography (EMG) connectors were inserted into the nuchal muscles. All electrode leads were connected to a head mount (Part #8201, 6 pins, 8 × 5 mm, Pinnacle Technology, Inc.) and sealed with dental acrylic HydroC (Dentsply, Buenos Aires, Argentina). While anesthetized, mice received

subcutaneously one dose of antibiotic (enrofloxacin, 85 mg/kg; John Martin Inc., Argentina) co-injected with analgesic (meloxicam, 5 mg/kg; John Martin Inc., Argentina). After surgeries, mice were administered with analgesic (tramadol, 20 mg/ml; Panacea Inc., Argentina) in their drinking water bottle. No changes in animal weights were observed from the day electrodes were implanted until the last day of EEG/EMG recordings (Table 1).

From day 14 post-surgery, each implanted animal was placed in the acrylic cylinder for habituation to the registration arena for periods of 2–4 h per day in the presence of ad libitum food and water. One week after the habituation period, the animals were placed in the acrylic cylinder at 15–16 h. On the day of registration, connecting them to the pre-amplifier unit (Part # 8202-SL, Pinnacle Technology, Inc.) rigidly attached to the mouse head mount provided 1st-stage amplification (100×) and initial high-pass filtering (1st-order 0.5 Hz for EEG and 10 Hz for EMG). All signals were routed to the conditioning/acquisition system (Data Conditioning & Acquisition System # 8206, Pinnacle Technology, Inc.) via a tether and low-torque commutator. Recording signals were further fifty-fold amplified, additional high-pass filtering, and an 8th order elliptic low-pass filter (50 Hz EEG and 200 Hz EMG). The signals were then sampled at 200 Hz, digitized using a 14-bit analog to digital converter and routed to a PC-based acquisition and analysis software package via USB. During offline analysis, awake stage was characterized by a preponderance of low amplitude, high frequency signals in the EEG signals combination with a highly variable muscle tone from electrodes inserted into the animal's neck (EMG). It was common to simultaneously observe abundant muscle activity on the EMG. During REM sleep clear peaks at theta-band frequencies (θ, 5–8 Hz) with no EMG activity were recorded. No REM sleep stage was characterized by unchanging muscle-related EMG activity and high power activity at low frequency bands, as δ-band [0.1–3.5 Hz].

Statistical analysis and data presentation

Data were stored for off-line analysis using Clampfit (pCLAMP 10.0, Molecular Devices, CA, USA). Comparisons between groups were carried out using OriginPro 9.1.0 (Origin lab.com, MA, USA). Normality and equal variance test were performed prior to ANOVA comparisons using Origin Pro 9.1.0. No sample calculation was performed. Data is presented as mean ± standard error of the mean. Data values that showed more/less than two times the standard deviation from the mean were excluded. Statistics were performed using *t* test, ANOVA, RM ANOVA, and non-parametrics test (Mann-Whitney Rank Sum Test and Kruskal-Wallis ANOVA on Ranks) when applicable. LSD Fisher's, Holm-Sidak's, or Tukey test's post hoc test were used to test statistical significance. Number of cells recorded is shown

Table 1 Animal weight from the day electrodes were implanted until the last day of EEG/EMG recordings

	Day 1: implanting electrodes	Day 14	Day 21	Day 30
Animal weight (gr.)	31 ± 1.2 (9)	31 ± 0.8 (9)	31 ± 0.9 (9)	32 ± 0.9 (9)

No significant differences were found comparing the weights of the animals throughout the experiment (one-way ANOVA; $F_{(3,32)} = 0.1, p = 0.9$)

throughout the text as “n=.” Differences were considered significant if $p < 0.05$.

Drugs and toxins

TTX was purchase from Alomone Labs. (Israel). Bicuculline, caffeine, cocaine, CNQX, DL-AP5, TEA, and salts used were purchased from Sigma-Aldrich (Argentina).

Results

Psychostimulant administration schedule and doses used in this work were based on previous studies published by our research group (Muñiz et al. 2016, 2017). Mice were injected with a mixture of cocaine and caffeine (PACO-like binge), whose composition resembles previously analyzed “cocaine pasta base” samples (Coc 10 mg/kg + Caf 5 mg/kg; see Muñiz et al. 2016, 2017). In addition, separate administrations of caffeine (5 mg/kg) or cocaine (10 mg/kg) were performed to elucidate the effects of their combination. Psychostimulants were administered in a binge-like form (i.e., three injections, 1 h apart) following an acute or chronic protocol (see Materials a Methods).

Characterization of both H-type and T-type currents in thalamocortical ventrobasal neurons 24-h after acute binge treatments

We studied H and T-type currents (I_H , I_T) in ventrobasal ThCo neurons 24-h after the acute administration of psychostimulants: saline (control), cocaine+caffeine (“PACO”-like binge), cocaine, and caffeine (Fig. 1).

I_H was pharmacologically isolated as described in Materials and Methods. I_H elicited by a hyperpolarizing pulse from -40 to -100 mV was markedly suppressed by its specific channel blocker ZD7288 (Fig. 1a). Characterization of activating and deactivating I_H currents revealed that an acute “PACO”-like binge was associated with a significant increase of the I_H current density (two-way RM ANOVA, $p < 0.05$), whereas the voltage-dependency of activation remained unaltered (Fig. 1b and c). Activation kinetics were best fitted by a double-exponential function and revealed no changes (not shown). However, a cocaine binge also increased I_H , whereas a caffeine binge did not produced any effect (ANOVA, $p < 0.05$, Fig. 1d). Similarly, Urbano et al. (2009) reported

an increase of I_H in VB neurons 1 h after an acute binge of cocaine. Therefore, I_H alteration observed 24-h after an acute “PACO”-like binge could be attributed to cocaine effects.

I_T was pharmacologically isolated as described in the “Materials and Methods” section. I_T elicited by a depolarizing pulse from -100 to -40 mV was blocked by its specific channel blocker TTA-A2 (Fig. 1e). Analysis of current-voltage relationship (I-V curves) showed that the I_T current density was not affected 24-h after an acute “PACO”-like binge (Fig. 1f and g). However, both cocaine and caffeine binges (separately administrations) increased the I_T current density (ANOVA, $p < 0.05$, Fig. 1h). Similarly, Urbano et al. (2009) reported an increase of I_T in VB neurons 1 and 24-h after an acute binge of cocaine. Our results suggested that the combined administration of cocaine and caffeine (“PACO”-like binge) prevented the increase of I_T that was observed in separately administrations of cocaine or caffeine.

HCN channels have been described to interact with T-type calcium channels (Fan et al. 2017) and they are key channels modulating the resting membrane potential (RMP) in thalamocortical neurons (Meuth et al. 2006; Budde et al. 2008). Figure 2a shows that the RMP was depolarized by ~ 10 mV after PACO-like and cocaine binges (ANOVA, $p < 0.05$), according to the observed increase of I_H current density.

Activation/deactivation dynamic of I_H intertwined with T-type calcium channels activation after membrane potential hyperpolarization (Jahnsen and Llinás 1984a, b), modulating the amplitudes and duration of low-threshold spikes (LTS). In order to study the functional interaction between I_H and I_T , we used a rebound protocol (-100 or -200 pA for 500 ms). LTS refer to large membrane depolarizations mediated by an increase of T-type calcium conductance, T-type channels open when the membrane potential is released from hyperpolarization at the end of a current step, as seen in VB neurons recorded under current clamp recording mode (Fig. 2b). The steady hyperpolarization current step also revealed the activation of I_H current that underlied a “sag” in the voltage response of VB neurons (Fig. 2b). Note how in the presence of Ni^{2+} , an unmask component related to I_H current-deactivation also contributes to rebound bursting (Fig. 2b). As seen in Fig. 2c, the specific blocker ZD7288 of I_H prevented this “sag” formation and delayed the LTS response. Upon release from membrane hyperpolarization, the averaged amplitude of LTS in VB neurons was larger after an acute “PACO”-like binge in comparison to other treatments (ANOVA, $p < 0.05$, Fig. 2d

and e). These results suggested that, in response to a hyperpolarizing input, VB neurons solely exhibit increased T-type calcium-mediated, low-threshold spike (LTS) amplitudes when cocaine was administered in combination with caffeine.

Acute “PACO”-like binge administration alters biophysical properties of T-type voltage-gated calcium channels

So far, our results suggest that acute “PACO”-like binge administrations prevented the increase of I_T that was observed after separately administrations of cocaine or caffeine (Fig. 1f–H). However, upon release from membrane hyperpolarization, only VB neurons that underwent an acute “PACO”-like binge treatment exhibited an increase of LTS amplitudes (Fig. 2). Therefore, we studied voltage and time dependence of T-type voltage-gated calcium currents in VB neurons comparing control vs. “PACO”-like binge acute treatments.

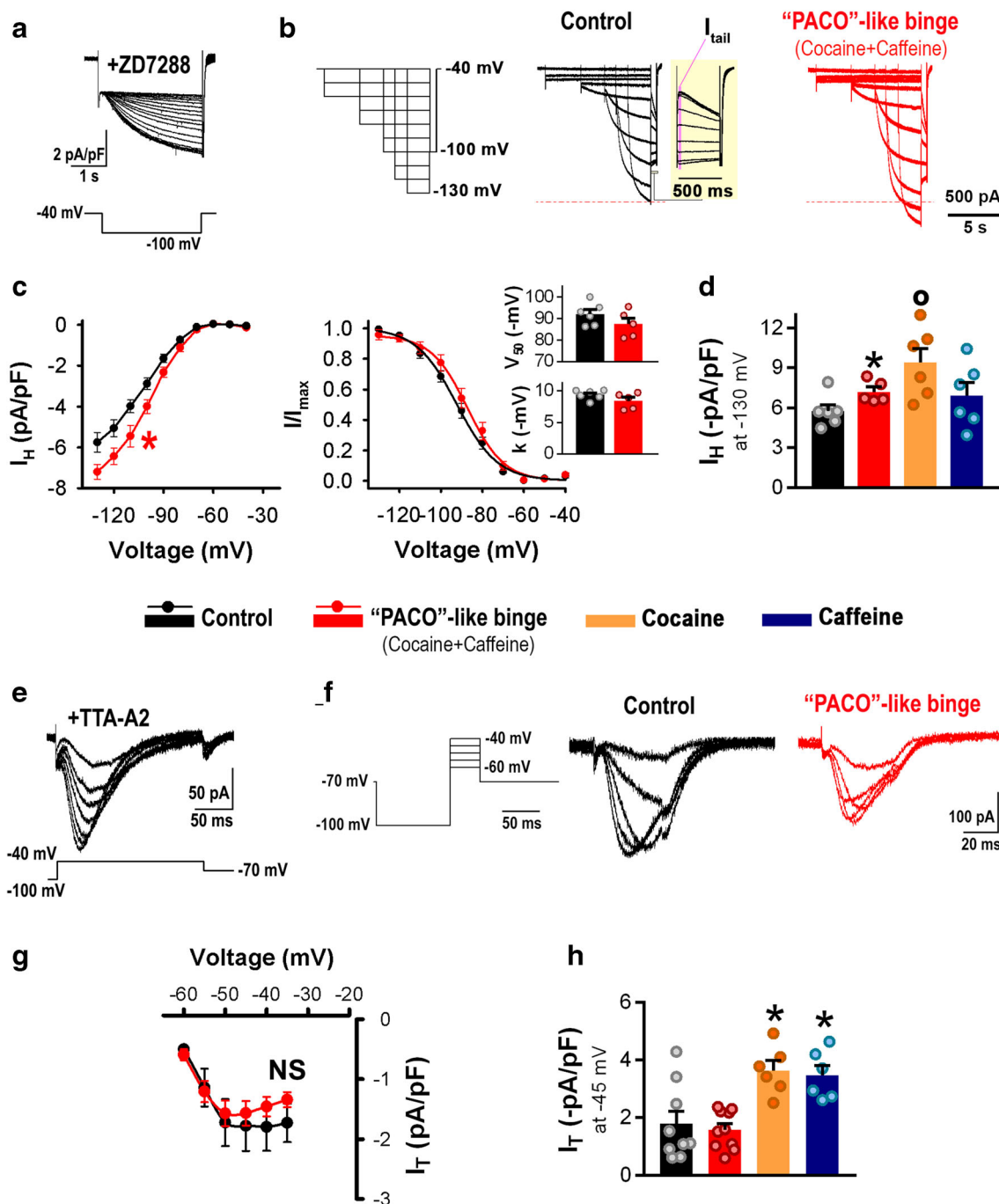
The voltage-dependent activation of I_T was determined by hyperpolarizing the holding potential to -110 mV for 500 ms and then progressing in 5 mV depolarizing steps towards T-type channels activation, as shown normalized current traces (I/I_{\max}) depicted in Fig. 3a. Peak current conductance for each holding step was normalized to the maximally elicited current conductance (G/G_{\max}) represented steady-state activation (SSA) of I_T for control (black dots) and “PACO”-like binge (red dots) treatments. Average values were plotted against its respective holding pulse potential and fitted using a Boltzmann equation (Fig. 3b). The V_{50} parameter was -65.2 ± 1.5 mV ($n = 10$) in control compared to -60.7 ± 1.7 mV ($n = 6$) after a “PACO”-like binge treatment. In addition, the slope factor k increased after a “PACO”-like binge (2.3 ± 0.2 mV vs. 4.0 ± 0.5 mV). SSA curves analysis showed that its midpoint potential (V_{50}) was significantly shifted by about ~ 5 mV after a “PACO”-like binge compared to control (Student’s t test, $t_{14} = -1.94$, $p < 0.05$). The approximate RMP for control (~ -70 mV, black symbols/lines) and “PACO”-like binge (~ -60 mV, red symbols/lines) groups are shown on the voltage axis of Fig. 3b. Thin lines showed interpolating RMP values towards Y-axis, obtaining the activable fraction of deactivated I_T . In control conditions (black line), a ~ 0.25 fraction of I_T would be activated at holding potentials within close range to resting membrane potentials. However, after acute “PACO”-like binges, a ~ 0.55 fraction of I_T would be activated at observed resting membrane potential values.

The steady-state inactivation (SSI) of the T-type Ca^{2+} current was determined by hyperpolarizing command potentials progressing at -5 mV increments, starting from -45 to -110 mV pre-pulse potentials for 500 ms and then stepping to the test potential (-50 mV). Peak currents for each step were normalized to the maximally elicited currents (I/I_{\max} , Fig. 3c) and average values were plotted against its respective pre-pulse holding potential for control (black dots) and

“PACO”-like binge treatment (red dots) (Fig. 3d). The inactivation data was fitted to a Boltzmann equation. The SSI V_{50} value changed from -85.5 ± 1.4 mV ($n = 11$) in controls to -78.7 ± 1.0 mV ($n = 6$) after “PACO”-like binges; no change in the slope factor k was observed (-5.3 ± 0.3 mV vs. -5.6 ± 0.4 mV). The SSI midpoint potential (V_{50}) was significantly shifted by about ~ 7 mV after a “PACO”-like binge compared to control (Student’s t test, $t_{15} = -3.2$, $p < 0.05$). The observed depolarizing shift between steady-state inactivation curves suggested an increment in the T-type Ca^{2+} channel availability. Thus, we concluded that an acute “PACO”-like binge increased the fraction of deactivated T-type Ca^{2+} channels (i.e., availability) near resting membrane potentials. For instance, a depolarizing step from a holding potential of -110 mV in which all T-type Ca^{2+} channels were fully deactivated (see orange bar showed on the left, Fig. 3d) showed no changes in I_T current density between control and “PACO”-like binge treatments (Fig. 3e). However, average I_T current density elicited from a holding potential of -70 mV were 3-fold bigger after a “PACO”-like binge (Fig. 3e), as expected according to the shift in the steady-state inactivation observed in Fig. 3d (see the fraction of deactivated channels indicated by the light blue bar).

Overall, our results suggested that after an acute “PACO”-like binge, a larger fraction of T-type Ca^{2+} channels would be deactivated after membrane hyperpolarization by an inhibitory input in comparison to control (i.e., a “PACO”-like binge increases the availability of T-type Ca^{2+} channels, Fig. 3c and d). In addition, the depolarizing effect of a “PACO”-like binge on the RMP would increase the activable fraction of deactivated T-type channels when the membrane potential suddenly reached its resting value at the end of the inhibitory input (Fig. 3a and b), favoring the generation of large LTS-associated Ca^{2+} transients, as shown above on Fig. 2 (d and e).

T-type Ca^{2+} channels operate in a subthreshold voltage range, with an overlap between activation and steady-state inactivation curves that produces a voltage range where a subset of T-type channels is constitutively active (i.e., steady-state current, I_{stst} or “window current”) (Hughes et al. 1999; Crunelli et al. 2005). Such “window current” can be observed as the “shaded region” underneath the activation and steady-state inactivation curves, which was shifted towards depolarizing potentials after an acute “PACO”-like binge (Fig. 3f, inset). The “window current” was theoretically estimated using the fitting parameters of the steady-state inactivation and activation curves (see “Material and Methods”) (Bijlenga et al. 2000; Lambert et al. 2014). The amplitude of the “window current” after an acute “PACO”-like binge was ~ 3 times larger than the control (Fig. 3f and g- I_{peak}). Moreover, the range of its voltage dependency was broader than the control (Fig. 3f, $G-\Delta V_{50}$). Boxplots in Fig. 3f depict the RMP for both control and “PACO”-like binge treatments. Interestingly, the “window current” increased ~ 3 –4 times at



the RMP after an acute “PACO”-like binge compared to control. Therefore, after an acute “PACO”-like binge, a large subset of T-type Ca^{2+} channels should be constitutively active at RMP compared to control, leading to a stationary Ca^{2+} influx and a persistent enhancement of $[\text{Ca}^{2+}]_i$.

Acute “PACO”-like binge administration alters intracellular calcium dynamics

To further confirm our findings, we investigated whether acute “PACO”-like binges lead to detectable changes in

intracellular Ca^{2+} concentration. Ratiometric Fura-2-based calcium imaging was performed concurrently with whole-cell recordings in VB neurons (Di Guilmi et al. 2014; Rozas et al. 2017; Rankovic et al. 2010). We determined the basal $[\text{Ca}^{2+}]_i$ and used an inhibitory current step (-200 pA for 500 ms) to measure Ca^{2+} transients (LTS) associated to H- and T-type currents (Fig. 4a). We used a K-gluconate/EGTA free intracellular solution in current-clamp configuration and an artificial cerebrospinal fluid (ACSF) with TTX, TEA, and synaptic blockers (AP5, CNQX, and bicuculline) to preclude the activation of voltage-gated sodium and potassium

Fig. 1 Characterization of H and T-type currents 24-h after acute binge treatments in thalamocortical ventrobasal neurons. **a** Blocking effect of an HCN specific blocker, ZD7288 (30 μM). HCN-mediated current (I_{H}) was evoked by an hyperpolarizing voltage step from a holding potential (V_{H}) of -40 to -100 mV (in an ACSF + 3 μM TTX, 10 mM TEA, 0.5 mM BaCl_2 , 0.1 mM CdCl_2 , 50 μM DL-AP-5, 20 μM CNQX, 50 μM Bicuculline). Current traces show time course of ZD7288 bath application (1 trace/min), reaching its maximum blocking effect after ~ 13 min. **b** I_{H} activation protocol (left plot) comparing VB neurons from control (center plot) vs. “PACO”-like binge treated mice (right plot), using a protocol that changed V_{H} from -40 to -130 mV, at 10 mV voltage steps. Duration of each hyperpolarizing pulse was shortened as the potential values became more negative, as previously described (Zobeiri et al. 2018, 2019). Average current traces are shown. Inset, tail currents were measured at -100 mV. **c** Average current-voltage relationship (I-V curve, left plot) and steady state of activation (SSA, right plot) curve for control (black, $n = 6$) vs. “PACO”-like binge (red, $n = 5$) treatments. SSA curves were fitted to the Boltzmann equation: $I/I_{\text{max}} = 1 / (1 + \exp. ((V - V_{50}) / k))$; where V is the membrane holding potential of the prepulse, V_{50} is the membrane potential in which half of I_{H} is activated, and k is the slope or “slow factor.” Right bar plots representing average V_{50} and k , including dots corresponding to individual data points. *Significantly different from control, $p < 0.05$. Two-way RM ANOVA, testing voltages (-100 to -130 mV, $F_{(3,27)}$: 171.46) and treatments ($F_{(1,27)}$: 6.42). There was not a statistically significant interaction between applied voltage values and treatments. **d** Bar plots comparing the mean I_{H} density at -130 mV for controls ($n = 6$), “PACO”-like administration ($n = 5$) and administration of either cocaine ($n = 6$) or caffeine ($n = 6$). *Significantly different from control, $p < 0.05$, Student’s t test, $t_9 = -2.330$. ^oSignificantly different from control and caffeine, $p < 0.05$, ANOVA, $F_{3,19} = 3.736$. **e** Blocking effect of an T-type specific blocker, TTA-A2 (10 μM). T-type current (I_{T}) was evoked by a depolarizing pulse from a $V_{\text{H}} = -100$ mV to -40 mV (in an ACSF + 3 μM TTX, 10 mM TEA, 50 μM DL-AP-5, 20 μM CNQX, 50 μM Bicuculline). Current traces showing time course of TTA-A2 bath application (1 trace/100 s), reaching its maximum blocking effect after ~ 12 min. **f** I_{T} activation protocol comparing VB neurons from control vs. “PACO”-like binge treated mice, using a protocol of holding potentials from -100 mV (100 ms) to -40 mV (50 ms), at 5 mV voltage steps. Average traces are shown. **g** Average current-voltage relationship (I-V curve) for control ($n = 9$) and “PACO”-like binge ($n = 10$) treatments. NS, no significantly difference between treatments ($p > 0.05$, two-way RM ANOVA). **h** Bar plots comparing mean I_{T} density (including dots corresponding to individual data points) at -45 mV for controls ($n = 9$), “PACO”-like binge ($n = 10$) and administration of either cocaine ($n = 6$) or caffeine ($n = 6$). *Significantly different from control and “PACO”-like binge, $p < 0.001$. ANOVA. $F_{3,27} = 9.574$.

currents. Ratiometric $[\text{Ca}^{2+}]_i$ indicator Fura-2 (0.5 μM) was added to the intracellular solution and VB neurons were allowed to passively reach a steady-state filling after gaining access to the cytoplasm for 5–10 min. Figure 4b shows digital images of a single VB neuron after a “PACO”-like binge treatment, which represent the raw 380 nm fluorescence intensity and the pseudocolor representation of the fluorescence ratio (340 nm/380 nm) at the resting (baseline) and during the inhibitory current step (LTS). $[\text{Ca}^{2+}]_i$ was determined from background-subtracted ratio values (340 nm/380 nm) as previously described by (Usachev et al. 1993; Rankovic et al. 2010; Di Guilmi et al. 2014). Figure 4c shows averaged $[\text{Ca}^{2+}]_i$ values for the baseline period before stimulus

presentation (typically ~ 7 s, $[\text{Ca}^{2+}]_{\text{basal}}$). In order to avoid calcium-induced calcium release mechanisms, internal calcium stores were depleted after exposing some neurons to bath-applied caffeine (20 mM; Usachev et al. 1993) for 10 min before applying the imaging protocol after reaching baseline $[\text{Ca}^{2+}]_i$ levels of the recorded VB neuron (+caffeine, Fig. 4c). The basal level of $[\text{Ca}^{2+}]_i$ was increased ~ 3 times after acute “PACO”-like binges (ANOVA, $p < 0.05$). This increase is still observed after depleting internal calcium stores (~ 2 times; Mann-Whitney, $p < 0.05$), according to the observed increase of T-type “window currents” (Fig. 3f). No differences were observed after separately administrations of cocaine or caffeine. Figure 4d depicts a typical response of a VB neuron during an inhibitory current step for control and “PACO” like binge treatments. The raw intensity values for the individual wavelengths (340 and 380 nm) resulted in a maximal crossover (and, hence, ratio value) when intracellular calcium levels increased (see right panel in Fig. 4b). Crossover of the individual wavelength intensities was indeed dramatic when the inhibitory current step pulse was applied to a neuron from a “PACO”-like binge treatment. Figure 4e shows the time course of averaged $[\text{Ca}^{2+}]_i$ dynamics, whose basal level was increased after a “PACO”-like binge as seen in Fig. 4c. Indeed, the rise in $[\text{Ca}^{2+}]_i$ was abrupt after the stimulus presentation to neurons acutely treated with “PACO”-like binges and subsequently returned to baseline (Fig. 4e). Figure 4f depicts the average of peak $[\text{Ca}^{2+}]_i$ values obtained during hyperpolarizing current steps ($[\text{Ca}^{2+}]_{\text{LTS}}$). No differences were observed after separately administrations of cocaine or caffeine. Regardless of bath-applied caffeine, $[\text{Ca}^{2+}]_{\text{LTS}}$ was increased after acute “PACO”-like binges.

Increase of basal $[\text{Ca}^{2+}]_i$ mediated by an acute “PACO”-like binge treatment modulates the biophysical properties of T-type voltage-gated calcium channels

Since an acute “PACO”-like binge administration increased the basal $[\text{Ca}^{2+}]_i$ (Fig. 4c) and prevented the increase of I_{T} that was observed after separately administrations of cocaine or caffeine (Fig. 1f–h), we hypothesized that T-type Ca^{2+} channels might be partially blocked by a basal increase of $[\text{Ca}^{2+}]_i$ after a acute “PACO”-like binge.

In order to evaluate our hypothesis, we studied the T-type Ca^{2+} current-voltage relationship (I-V curve) after intracellular dialyzing of the recorded neuron with 0.5 or 10 mM EGTA (a calcium chelator included in the pipette solution) comparing control and acute “PACO”-like binge treatments (Fig. 5a–c) (Marty and Neher 1985; Roberts 1993; Deisseroth et al. 1996). Under control conditions, no significant changes in I-V curves were observed between 0.5 and 10 mM EGTA (Fig. 5a, b) (two-way RM ANOVA, $p > 0.05$). However, after an acute “PACO”-like binge, increasing the EGTA concentration

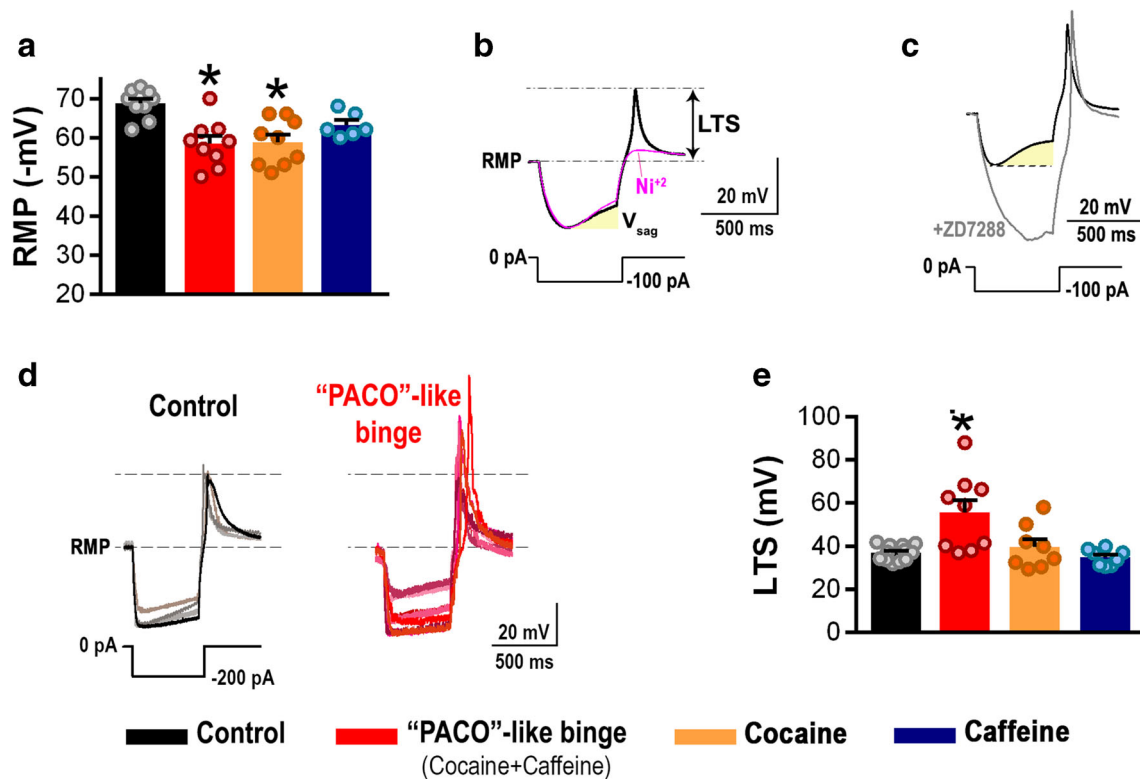


Fig. 2 An acute “PACO”-like binge administration increased low-threshold spike (LTS) amplitude in VB neurons. **a** Resting membrane potential (RMP) recorded in VB neurons 24 h after all binge groups (control, $n = 9$; “PACO”-like, $n = 9$; cocaine, $n = 9$; or caffeine, $n = 6$). *Significantly different from control, $p < 0.05$, ANOVA. $F_{2,24} = 10.98$. **b** Representative trace of a VB neuron recorded in current-clamp (in an ACSF +3 μM TTX, 10 mM TEA, 50 μM AP-5, 20 μM CNQX, 50 μM Bicuculline). Low-threshold spikes (LTS) were triggered by a

hyperpolarizing square pulse (-100 pA). LTS were blocked by nickel (Ni^{2+} , 100 μM). **c** Blocking effect of the specific blocker of HCN channels, ZD7288 (30 μM), in current-clamp recording mode. **d** Overlapping LTS responses for controls and “PACO”-like binge treatments. LTS were triggered by a hyperpolarizing square pulse (-200 pA). **e** Changes in LTS amplitude for controls ($n = 12$), “PACO”-like ($n = 9$), cocaine ($n = 8$), and caffeine ($n = 8$) treatments. *Significantly different from other treatments, $p < 0.05$, Kruskal-Wallis ANOVA on Ranks, $H_3 = 11.82$

from 0.5 to 10 mM shifted the peak of the I-V curve by ~ 12 mV in the hyperpolarizing direction (-46.7 ± 1.0 mV vs. -58.3 ± 1.0 mV) and increased its current density by $\sim 40\%$ (-4.2 ± 0.8 pA/pF vs. -6.0 ± 0.6 pA/pF) (two-way RM ANOVA, $p < 0.01$, Fig. 5a and c). These results support the idea that the basal increase of $[\text{Ca}^{2+}]_i$ partially blocked and shifted the voltage dependence of T-type Ca^{2+} channels. These results also suggested that the separately effect of cocaine and/or caffeine on T-type currents (Fig. 1h) was uncovered when 10 mM EGTA was included in the recording pipette solution (Fig. 5c).

Furthermore, biophysical properties of activation and inactivation were studied after dialyzing neurons with 10 mM EGTA. We have compared these experiments with those presented in Fig. 3 (b and d), which were performed with a 0.5 mM-EGTA in the pipette solution (Fig. 5d–g). Under control condition, both activation and steady-state inactivation curves were not affected by increasing the EGTA concentration in the pipette solution from 0.5 to 10 mM (Fig. 5d). Figure 3 (b and d) showed that both activation and steady-state inactivation curves were shifted towards depolarizing potential after an acute “PACO”-like

binge compared to control (0.5 mM EGTA was included in the pipette solution). Importantly, increasing the EGTA concentration in the pipette solution to 10 mM prevented the depolarizing shift of both activation and steady-state inactivation curves (Fig. 5e) and their average midpoint potentials (V_{50}) resemble those determined in control conditions (Fig. 5f, g). Similar behavior was observed for the activation slope factor k (Fig. 5f, g). Table 2 summarizes V_{50} and slope factor k average values in dialyzed neurons with either 0.5 or 10 mM EGTA for both control and “PACO”-like binge treatments. Our results involved $[\text{Ca}^{2+}]_i$ -dependent mechanisms that modulate the biophysical properties of T-type Ca^{2+} channels, which critically link these calcium channels to their physiological functions.

Chronic “PACO”-like binge administration alters I_H current mediated by HCN channels

In contrast to acute binges, chronic “PACO”-like binges reduced I_H density and shifted the membrane potential in which half I_H was activated (V_{50}) towards hyperpolarizing values (two-way RM ANOVA, $p < 0.001$, Fig. 6a–c). Consistently,

we quantified using RT-qPCR that levels of HCN2 mRNA in the VB nucleus decreased by ~55% ($n = 6$, Student's t test, $t_{10} = 3.42$, $p < 0.01$; data not shown). The acute effect of cocaine on I_H density was no longer maintained when the administration became chronic (Fig. 6d). On the other hand, the chronic "PACO"-like binges did not inhibit but enhanced voltage-gated T-type currents density (ANOVA, $p < 0.05$; Fig. 6e and f). Furthermore, no differences in I_T density were observed when comparing with the chronic cocaine administration (Fig. 6f). Interestingly, acute effects of "PACO"-like binges in basal $[Ca^{2+}]_i$ levels were no longer maintained after chronic binges (Fig. 6g). These results support our findings about a partial blockade of the T-type current density by an intracellular $[Ca^{2+}]$ increase 24-h after an acute "PACO"-like binge, which returns to normal levels when the binge administration becomes chronic, uncovering solely cocaine effects on T-type currents (Fig. 6e and f).

Since we found no differences between LTS-associated Ca^{2+} transients after a chronic "PACO"-like binge respect to control, we assumed no apparent differences in biophysical properties of the T-type channel (Fig. 6h). In addition, the profound decrease of I_H density and the hyperpolarizing shift of its activating curve after a chronic "PACO"-like binge (Fig. 6a–c) would generate a weak depolarizing force hindering the opening of the T-type Ca^{2+} channels and the generation of LTS-associated Ca^{2+} transients.

Excitability of VB neurons 24-h after acute or chronic "PACO"-like binge administrations

H-currents tend to stabilize the resting membrane potential. The net effect of HCN channel activation is a decrease in the input resistance of the membrane (Magee 1998; Kase and Imoto 2012). Figure 7a shows a reduction of the input resistance in VB neurons 24-h after an acute "PACO"-like binge administration (Student's t test, $p < 0.05$), according to the observed increase of I_H density (Fig. 1b and c). Conversely, the input resistance increased 24-h after a chronic administration (Student's t test, $p < 0.05$), in line with the observed decrease of I_H density and the hyperpolarizing shift of its activation (Fig. 6a–c). Furthermore, we studied the characteristic voltage sag related to the level of I_H activation in response to a hyperpolarizing current step (-500 pA for 500 ms). As expected, the voltage sag ratio values were increased in VB neurons that underwent an acute "PACO"-like binge treatment (red trace). A significantly reduction in voltage sag ratios was observed 24-h after a chronic treatment (maroon trace, Fig. 7b; Student's t test, $p < 0.05$).

I_H -mediated alterations in membrane resistance will determine how the neurons respond to incoming stimulation (ie. level of voltage change) (Magee 1998; Kase and Imoto 2012). Therefore, membrane excitability was quantified by assessing the threshold and the number of APs with a current ramp

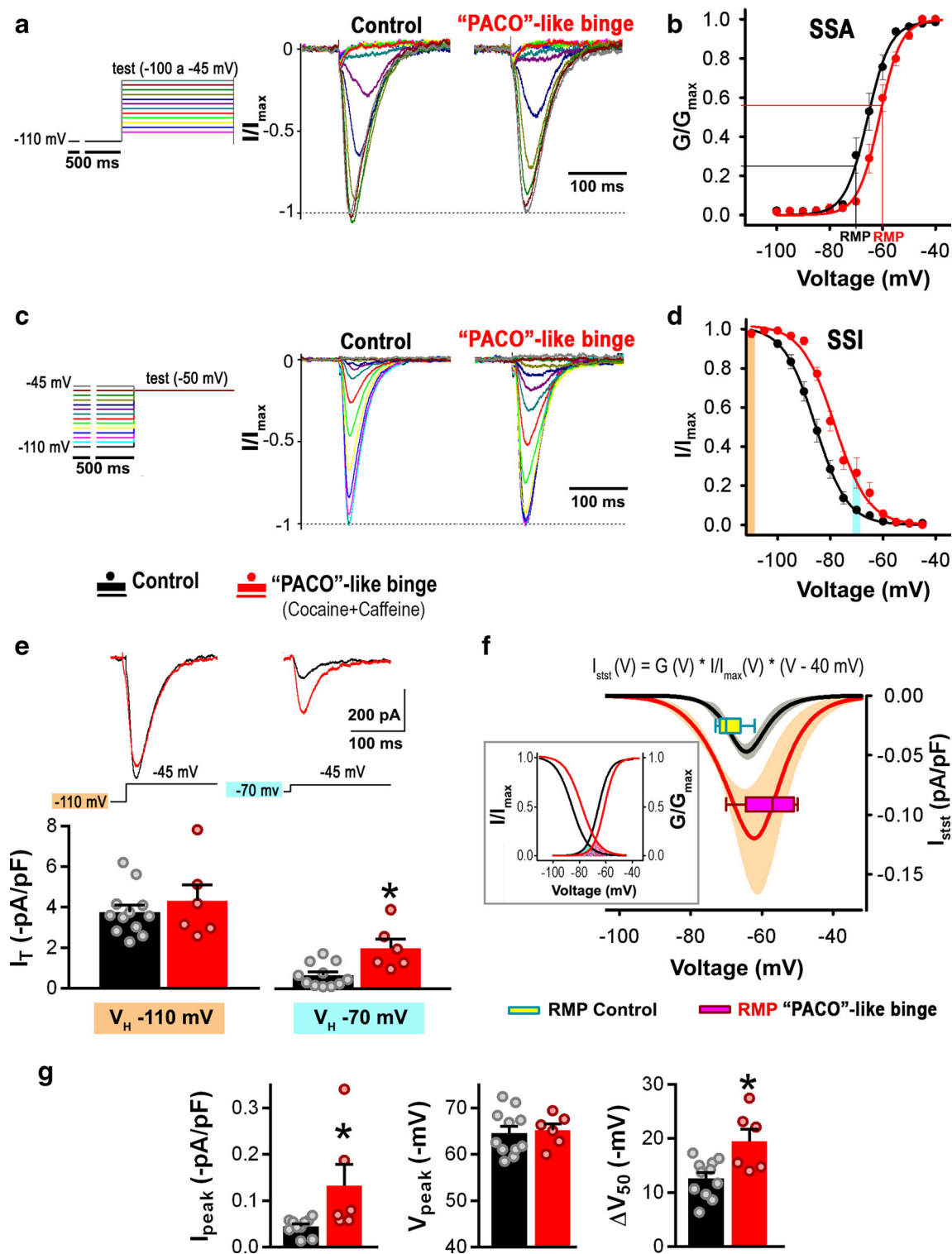
stimulus (ramp rate of 0.67 pA/ms) applied after hyperpolarizing the membrane (-200 pA for 50 ms) to activate H and T-type currents. Action potentials triggered by a LTS were called low-threshold action potentials (LT AP) and those triggered later were called high-threshold action potentials (HT AP) (Fig. 7c). Membrane excitability decreased 24-h after an acute "PACO"-like binge (compare left and middle trace and see the V_{sag} in Fig. 7c). The threshold of both LT AP and HT AP was depolarized by ~3.8 and 5.5 mV, respectively (Student's t test, $p < 0.05$; Fig. 7d). In addition, the action potential number of HT APs was decreased by ~60% (Student's t test, $p < 0.05$; Fig. 7e). Conversely, membrane excitability increased 24-h after a chronic "PACO"-like binge. The threshold of LT AP was hyperpolarized by ~3.3 mV (Student's t test, $p < 0.05$) and no change was observed in the threshold of HT AP (Fig. 7d). However, the action potential number of both LT AP and HT AP was increased by 56 and 48%, respectively (Student's t test, $p < 0.05$; Fig. 7e).

Overall, 24 h after an acute "PACO"-like binge administration, the enhancement of I_H density decreases the input resistance, diminishing the intrinsic membrane excitability. Conversely, the reduction of I_H density after a chronic administration increases the input resistance, allowing membrane potentials to move significantly closer to threshold, enhancing the intrinsic membrane excitability. The threshold of both LT AP and HT AP was depolarized after an acute "PACO"-binge administration, according to the depolarized RMP (Fig. 2a), likely resulting from the increase of not only I_H but also T-type "window current" (Fig. 1b–c, 3f–g). When the administration became chronic, the threshold of LT AP was hyperpolarized as it was reported by Urbano et al. (2009) for VB neurons after cocaine binge administration.

Can alterations at ventrobasal neurons by a chronic "PACO"-like administration affect sleep/awake phases during EEG/EMG recordings?

Our results showed that an acute "PACO"-like binge administration produced notorious alterations in the physiology of VB neurons that increased LTS-associated Ca^{2+} transients and decreased the membrane excitability. We observed homeostatic changes when the administration became chronic; such as a downregulation of basal $[Ca^{2+}]_i$ to normal levels and a drastic reduction of I_H , which not only reestablished the LTS-associated Ca^{2+} transients as observed in controls but also increased the membrane excitability to values even higher than control. In order to study the physiological impact of these chronic-mediated alterations on the sleep-wake transitions, we performed electroencephalography in mice 24-h after a chronic "PACO"-like binge.

We recorded EEG/EMG in mice 24 h after being systemically treated with chronic administration of cocaine+caffeine ($n = 5$ mice) and with the administration of vehicle, saline ($n =$



4 mice). We have programmed the last systemic drug administration 24 h before EEG/EMG recordings. Recordings started 2 h before light cycle change (that is, 18 h 2 h of turning off the light at 20:00 h) and lasted until 8 a.m. the following day. Percentages of time in the awake, NREM, and REM stages were plotted for every hour of recording

(Fig. 8) comparing animals chronically treated with the "PACO"-like binge versus vehicle. Greater awake percentage of time was observed after chronic "PACO"-like binges treatment compared to saline (Fig. 8a, b). One-way RM ANOVA comparison showed that treatment significantly affected awake times $F_{(1,7)} = 94.6$; $p < 0.001$ (Fig. 8a). Mean total

◀ **Fig. 3** Effects of acute “PACO”-like binge on T-type calcium current properties in VB neurons. **a** Steady-state activation (SSA) protocol of low-threshold T-type calcium currents. Holding potential (V_H) was maintained at -110 mV for 500 ms, then it was changed using square pulses from -100 to -45 mV in 5 mV steps. Average current traces for control ($n = 10$) and “PACO”-like binge ($n = 6$) groups are shown. **b** Average steady-state activation (SSA) values (and solid lines fitted to a Boltzmann equation) for control (black dots) and “PACO”-like binge (red dots) groups expressed as individual/maximum conductance ratio (G/G_{max}) as a function of holding voltage. The value of the resting membrane potentials (RMP) for both treatments is indicated on the abscissa axis. **c** T-type currents steady-state inactivation (SSI) protocol using a holding potential maintained at -110 mV for 500 ms, then it was changed using square pulses from -100 to -45 mV at 5 mV steps, followed by a holding square test pulse of -50 mV. Average current traces for control ($n = 10$) and “PACO”-like binge ($n = 6$) groups are shown. **d** Average steady-state inactivation (SSI) values (and solid lines fitted to a Boltzmann equation) for control (black dots) and “PACO”-like binge (red dots) groups expressed as individual/maximum current (I/I_{max}) as a function of holding voltage. Orange bar on the left showed 100% of T-type channels were de-inactivated. Light blue bar illustrates holding potential of -70 mV. Note how “PACO”-like binge values were 3-fold bigger than control. **e** **Above:** Representative T-type current traces for control (black line) or “PACO”-like binge (red line) treatment groups. Below: average I_T current density values were elicited from a V_H of either -110 mV (left) or -70 mV (right); same holding values are represented in 4D as orange and light blue bars, respectively. *Significantly different from control (Student’s t test; $t_{15} = 3.34$, $p = 0.002$; for control, $n = 10$ and for “PACO” like binge, $n = 6$). **f** Left inset: overlapping steady-state activation and inactivation curves of control and cocaine + caffeine obtained as Boltzmann fitting from (b) and (d). Note light blue and pink “shaded” colored areas representing the “window current” for control and “PACO”-like binge treatments, respectively. Right curve: I_T currents at the steady-state level [See the above equation used to calculate the theoretical “Window current”; $I_{T(stst)} = G(V_H) * I_T / I_{T,max} * (V_H) * (V_H \text{ at } -40 \text{ mV})$], without normalizing G , for each treatment. The black line represents the average currents in control, while the gray area around it representing its standard error. The red line and orange area represent values obtained after a “PACO”-like binge treatment. Boxplots indicated average resting membrane potential (RMP) for each treatment. **g** Comparison of key average parameters corresponding to the curves represented in (f). *Significantly different from control. Student’s t test; $t_{15} = 2.4$, $p = 0.01$; for control $n = 11$, for “PACO”-like binge $n = 6$)

awake time were also significantly different (Fig. 8b; Student’s t test, $df = 13$; $t = 4.5$; $p < 0.001$). On the other hand, NREM sleep percentage of time was reduced after chronic “PACO”-like binge treatment (Fig. 8c; RM ANOVA $F_{(1,7)} = 10.5$; $p < 0.05$). Mean total NREM reduction was also significantly different (Fig. 8d; Student’s t test, $df = 13$; $t = 2.6$; $p < 0.05$). There are no changes in REM sleep percentage of time (Fig. 8e; RM ANOVA $F_{(1,7)} = 0.8$; $p > 0.05$).

Discussion

This study provides evidence that acute and chronic administrations of a cocaine and caffeine mixture, resembling a sample of cocaine paste base or “PACO”, produce notorious alterations in intracellular calcium dynamics and dysregulate HCN-mediated and T-type conductances in thalamic

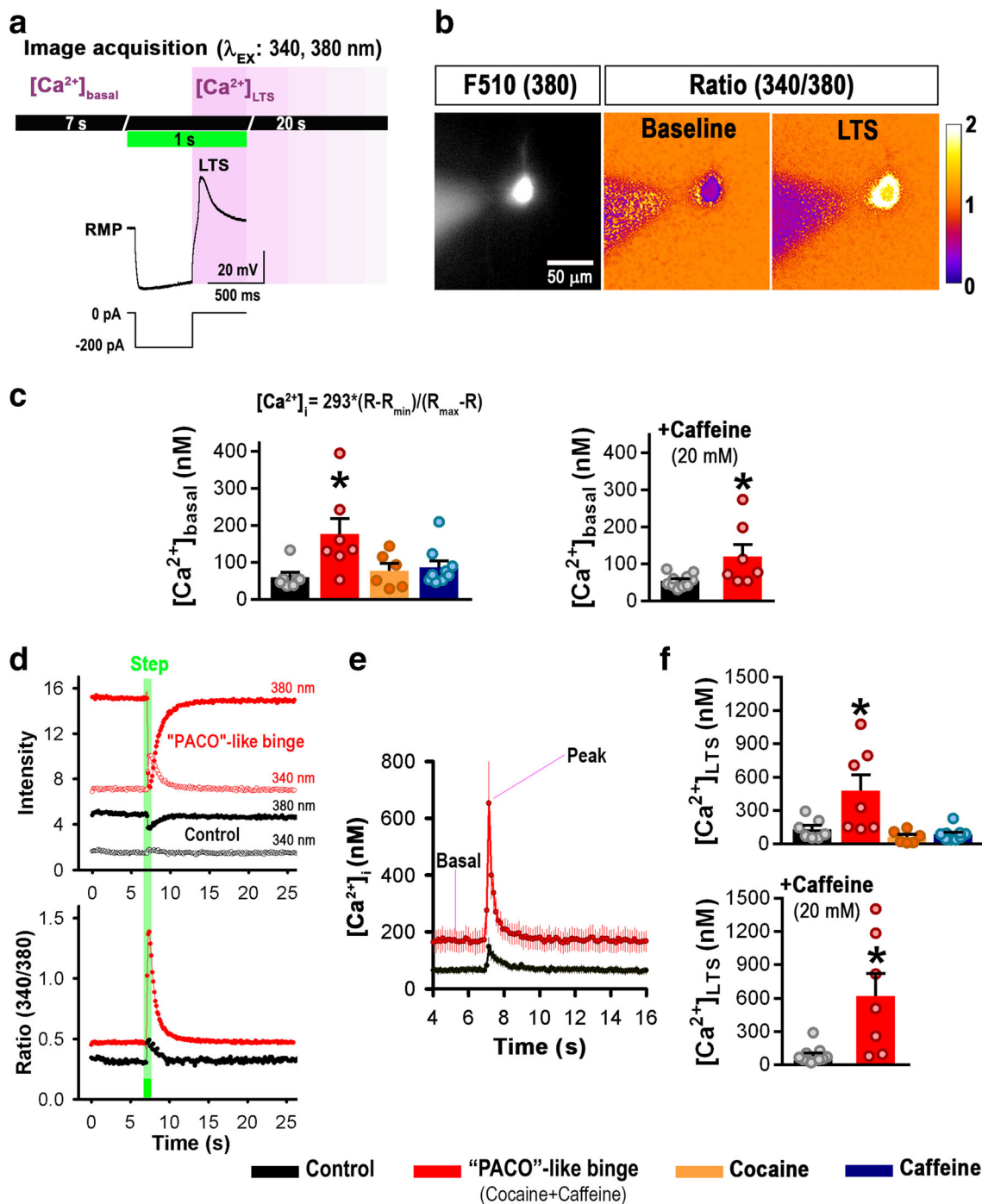
ventrobasal (VB) neurons of mice. All these changes ultimately modulated the membrane excitability, altering sleep-wake transitions.

Thalamic electrophysiology recordings have previously shown that brain rhythms (using electroencephalogram recordings) had a counterpart in the rhythmic oscillations and action potentials discharge that occur at single-cell level (Steriade and Amzica 1996). Altered plasma membrane expression of several voltage-gated ion channels of Ventrobasal (VB) neurons (specific thalamocortical neurons) has been proposed as the etiology of stimulants-mediated effects. Our group previously work showed how cocaine systemic administration mediated both hyperlocomotion and the increase of T-type calcium channel expression at thalamocortical VB neurons (Urbano et al. 2009; Bisagno et al. 2010; Goitia et al. 2013, 2016). Moreover, the increase of T-type and HCN currents, plus the enhancement of synaptic GABAergic activity induced by cocaine administration in mice, was suggested to “lock” the whole thalamocortical system into low frequencies in the EEG (Urbano et al. 2009). Thus, characterizing how effects of “PACO”-like administration affected VB neurons intrinsic properties allowed our group to dissect important underlining mechanisms of the described alterations of sleep-wake transitions during EEG recordings.

Alterations in $[Ca^{2+}]_i$ mediated by acute “PACO”-like binge treatments might be the key factor underlying changes on T-type and HCN channels at ventrobasal thalamic nucleus

The current density mediated by HCN channels (I_H) increased 24-h after an acute “PACO”-like binge administration with a concomitant depolarization of the resting membrane potential (RMP), similarly to an acute binge of cocaine. In line with our experiments, I_H upregulation has been previously described in VB neurons 1-h after the administration of a cocaine binge (Urbano et al. 2009; Bisagno et al. 2010). Therefore, I_H alteration observed 24-h after an acute “PACO”-like binge could be attributed to cocaine effects.

T-type Ca^{2+} current (I_T) density decreased 24-h after an acute “PACO”-like binge administration. Conversely, separately administration of cocaine or caffeine increased I_T density similar to previously reported for an acute binge of cocaine (Urbano et al. 2009). Our experiments showed an increase of basal $[Ca^{2+}]_i$ in VB neurons after an acute “PACO”-like binge treatment. Interestingly, we revealed a calcium-dependent inhibition of I_T after dialyzing the neuron with 10 mM EGTA, unmasking cocaine and/or caffeine effects on I_T . In line with our experiments, it has been described that the presence of ionomycin (an ionophore that allows calcium channels to enter the cell) partially blocked T-type currents in primary cultures of dorsal root ganglia neurons (Cazade et al.



2017). Furthermore, other authors have shown that calmodulin and the T-type, $Ca_v3.1$ channels are constitutively associated, and $[Ca^{2+}]_i$ influx through the channel pore was sufficient to activate α - Ca^{2+} -calmodulin kinase II (Asmara et al. 2017). A direct regulation of T-type $Ca_v3.2$ channels by Ca^{2+} -calmodulin kinase II has also been described (Welsby et al. 2003).

We found that T-type Ca^{2+} channels in VB neurons were dynamically regulated by changes in $[Ca^{2+}]_i$. Indeed, 24-h after an acute "PACO"-like binge treatment, we observed a

rightward shift of both the steady-state inactivation and activation curves of T-type Ca^{2+} channels; which was prevented by the addition of 10 mM EGTA to the pipette solution. These results further described that steady-state properties of T-type channels are finely modulated by basal $[Ca^{2+}]_i$ enhancements mediated by acute "PACO"-like binge administrations. Indeed, our results suggested that after an acute "PACO"-like binge, a large fraction of T-type Ca^{2+} channels would be deinactivated in response to an inhibitory input. In addition, the depolarizing effect of a "PACO"-like binge on the RMP

Fig. 4 Acute “PACO”-like binge increased intracellular basal calcium and LTS-associated Ca^{2+} transients in VB neurons. **a** Above, illustrating drawing of the acquisition protocol used to determine basal and LTS-associated $[\text{Ca}^{2+}]_i$ transients ($[\text{Ca}^{2+}]_{\text{basal}}$, $[\text{Ca}^{2+}]_{\text{LTS}}$). We used a hyperpolarizing current step (-200 pA for 500 ms) to elicit a LTS spike (in an ACSF + 3 μM TTX, 10 mM TEA, 50 μM AP-5, 20 μM CNQX, 50 μM Bicuculline). Below, representative LTS. Images were acquired 7 s before (baseline) and 20 s after the stimulation protocol (1 s duration). **b** Representative raw fluorescence emission image (510 nm) from a Fura-2-filled VB neuron excited at 380-nm wavelength (left) 24-h after a “PACO”-like binge treatment. A pseudo color scheme has been applied after calculating the fluorescence ratio $F(\text{Ratio}) = F_{340}/F_{380}$ at the resting (baseline, middle) and during the inhibitory current step (LTS, right). White scale bar represents size of recorded area. Scale bar on the right indicates with white as the highest and black as the lowest fluorescence ratio. **c** Left: basal intracellular calcium concentration ($[\text{Ca}^{2+}]_{\text{basal}}$) was calculated averaging $[\text{Ca}^{2+}]_i$ values for the baseline period (typically ~ 7 s), using the formula: $293 \cdot (R - R_{\text{min}}) / (R_{\text{max}} - R)$. R_{min} was the minimum ratio obtained in the absence of calcium and R_{max} is the highest ratio value obtained when Fura-2 is saturated and was calculated as previously described (Usachev et al. 1993; Rankovic et al. 2010; Di Guilmi et al. 2014). Mean \pm SEM values are presented for control ($n = 7$), “PACO”-like ($n = 7$), cocaine ($n = 6$), and caffeine ($n = 10$) treatments. *Significantly different from control, $p < 0.05$. Kruskal-Wallis ANOVA on Ranks, $H_3 = 8.65$. Right: Internal calcium stores were depleted applying caffeine (20 mM; Usachev et al. 1993) to the bath for 10 min before images acquisition (+ caffeine). Mean \pm SEM values are presented for control ($n = 10$), “PACO”-like ($n = 7$). *Significantly different from control, $p < 0.05$. Mann-Whitney, $U_{\text{Statistic}} = 14.0$. **d** Top: raw intensity values for 340- and 380-nm excitation wavelengths for a VB neuron after control and “PACO”-like binge treatments. See the baseline and the crossover of the individual wavelength intensities before and after the stimulus application (marked in green). Bottom: ratio values of these individual wavelength intensities that were calculated offline (Ratio[340/380]). **e** Time course of averaged $[\text{Ca}^{2+}]_i$ dynamics for control and “PACO”-like binge treatments (each one $n = 7$) before, during, and after the hyperpolarizing inhibitory current step stimulus. **f** Top: LTS-associated Ca^{2+} transients ($[\text{Ca}^{2+}]_{\text{LTS}}$) calculated as peak $[\text{Ca}^{2+}]_i$ obtained during the inhibitory current step. Mean \pm SEM values are presented for control (black; $n = 7$), “PACO”-like (red; $n = 7$), cocaine (yellow, $n = 6$) and caffeine (blue, $n = 9$) treatments. *Significantly different from other treatments, $p < 0.05$. Kruskal-Wallis ANOVA on Ranks, $H_3 = 13.19$. Bottom: $[\text{Ca}^{2+}]_{\text{LTS}}$ after applying caffeine (20 mM) to the bath for 10 min before images acquisition (+ caffeine). Mean \pm SEM values are presented for control (black, $n = 11$) or “PACO”-like (red, $n = 7$). *Significantly different from control, $p < 0.05$. Mann-Whitney, $U_{\text{Statistic}} = 7.0$

would increase the activable fraction of deinactivated T-type Ca^{2+} channels when the membrane potential suddenly reached its resting value at the end of this inhibitory input, and in combination with I_{H} current-deactivation would also favor the generation of large low-threshold spike (LTS)-associated Ca^{2+} transients. Our results are also consistent with previous reports, describing how intracellular Ca^{2+} released from internal stores finally shaped LTS in reticular thalamic neurons (Coulon et al. 2009). On the other hand, the observed increase of I_{H} density after an acute “PACO”-like binge administration would stabilize the resting potential of VB neurons (Meuth et al. 2006; Brennan et al. 2016; Zobeiri et al. 2019), enhancing even more the amplitude of LTS, given the

functional and physical association between HCN and T-type channels (Fan et al. 2017).

Solely, the acute administration of cocaine combined with caffeine (“PACO”-like binge) produced a large increase of basal $[\text{Ca}^{2+}]_i$ that persisted after 24-h; separately administration of these stimulants did not produce any effect on $[\text{Ca}^{2+}]_i$. Caffeine concentration (5 mg/kg) used in this work has been associated with caffeine brain levels in the tens of micromolar range (Heppert and Davies 1999; Goitia et al. 2016). Such caffeine concentration levels have been ascribed to adenosine receptor blockage (Fredholm 1995; Fredholm et al. 1999), rather than acting through the inhibition of phosphodiesterase (Aoyama et al. 2011), or the opening of ryanodine and IP_3 receptors (Garaschuk et al. 1997; Rankovic et al. 2010). Caffeine is a known activator of ryanodine receptors located in the endoplasmic reticulum (Rankovic et al. 2010; Usachev et al. 1993). We expect that each systemic administration of caffeine would produce a transient increment of intracellular $[\text{Ca}^{2+}]$ mediated in part by ryanodine receptors opening on thalamocortical/corticothalamic networks. Repetitive caffeine administration would sensitize ryanodine receptors, allowing them to be more sensitive to smaller cytosolic increments in $[\text{Ca}^{2+}]$ (Verkhatsky and Shmigol 1996). Indeed, bath application of caffeine (+ 20 mM) elicited three fold $[\text{Ca}^{2+}]$ levels after acute “PACO”-like binges. A new group of experiments are still needed in order to functionally link $[\text{Ca}^{2+}]_i$ transients after caffeine systemic administrations and the described dysregulation of HCN and T-type channels that we observed 24-h after acute/chronic “PACO”-like administration.

On the other hand, it has been reported that an acute cocaine dose (1 mg/kg) induced in vivo a large increase of $[\text{Ca}^{2+}]_i$ in the cortex of the rat brain (Du et al. 2006). Similarly, VB neurons exhibited high levels of $[\text{Ca}^{2+}]_i$ 1-h after an acute cocaine administration (3 injections, 15 mg/kg each, 1 h apart) (Rozas et al. 2017). However, our experiments were performed 24-h after the acute cocaine administration. We do not exclude the possibility that caffeine enhances the effect of cocaine leading to a dysregulation of $[\text{Ca}^{2+}]_i$ homeostasis. Indeed, our results showed that 24-h after an acute “PACO”-like binge administration, the calcium-dependent modulation of T-type biophysical properties resulted in a great increase of I_{T} -mediated “window currents,” suggesting that a large subset of T-type channels would be permanently opened at resting membrane potential, leading to a stationary Ca^{2+} influx and a persistent enhancement of $[\text{Ca}^{2+}]_i$. Moreover, it is known that calcium entry through T-type channels stimulates the release of calcium from intracellular compartments (Richter 2005).

However, when “PACO”-like binge administration became chronic, basal $[\text{Ca}^{2+}]_i$ returned to normal levels, where by I_{T} density was no longer inhibited, reaching enhanced values as observed after a chronic administration of cocaine. Likewise, Goitia et al. (2013) reported that thalamic VB

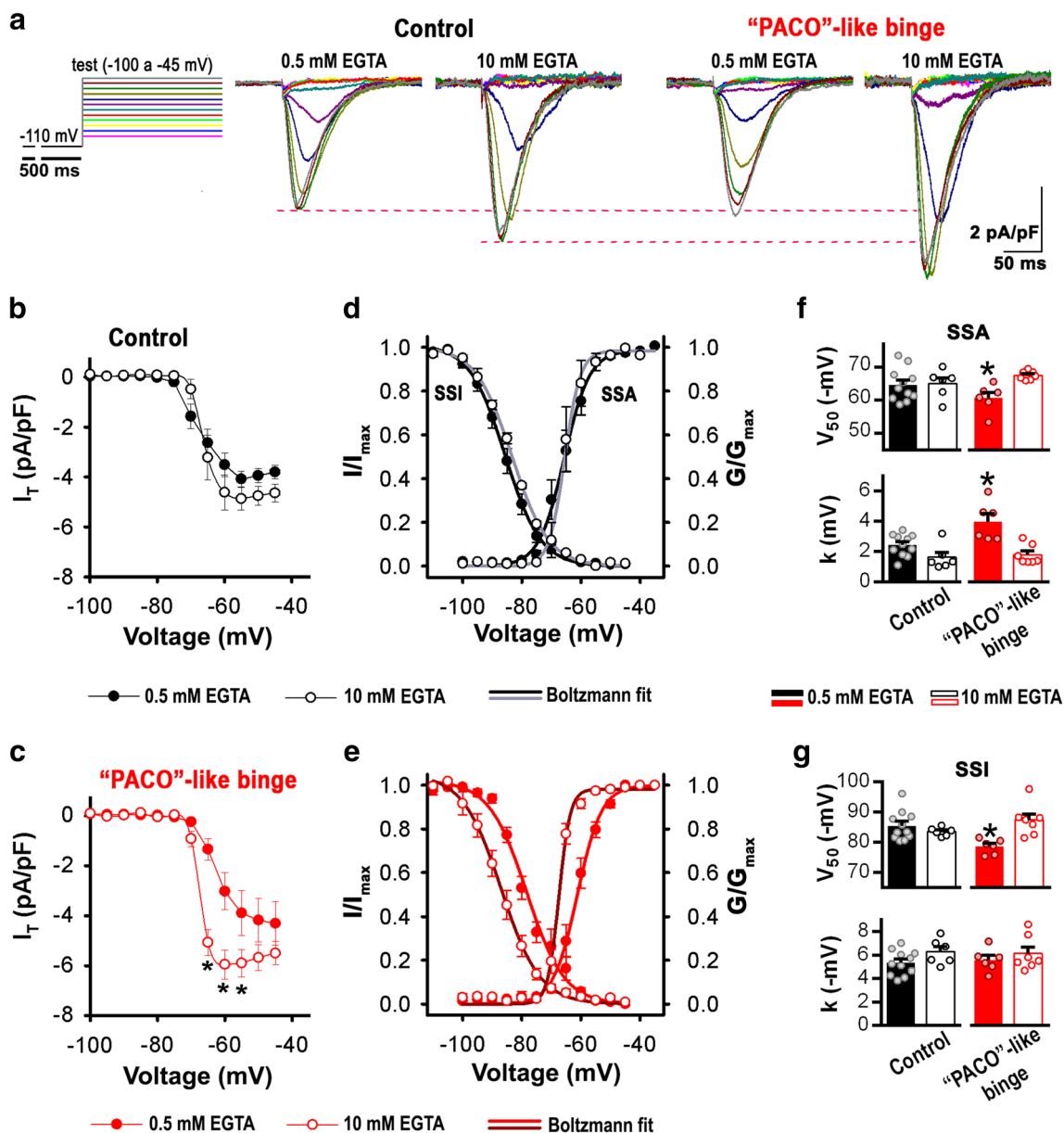


Fig. 5 Altered modulation of T-type voltage-gated calcium currents in ventrobasal neurons by intracellular calcium levels after an acute "PACO"-like binge treatment. **a** Left: Steady-state activation protocol (SSA). Center: average I_T traces from a control treated VB neurons recorded using EGTA 0.5 mM and 10 mM in the intracellular pipette solution. Right: Average I_T traces from a "PACO"-like binge treated VB neurons recorded using EGTA 0.5 mM and 10 mM in the pipette solution. **b** Current-voltage (I - V) curve of I_T currents from control treated VB neurons recorded using EGTA 0.5 mM (empty black dots; $n = 11$) or EGTA 10 mM (solid black dots; $n = 6$). No significant differences were observed ($p > 0.05$, two-way RM ANOVA). **c** Current-voltage (I - V) curve of I_T from "PACO"-like binge treated VB neurons recorded using EGTA 0.5 mM (empty red dots; $n = 6$) or EGTA 10 mM (solid red dots;

$n = 7$) in the pipette solution. *Significantly different from EGTA 0.5 mM, $p < 0.01$. Two-way RM ANOVA, testing voltages (-65 to -50 mV, $F_{(3,30)}: 16.17$) and treatments ($F_{(1,30)}: 9.92$). There was a statistically significant interaction between the applied voltages and treatments ($F_{(3,30)}: 6.04$). **d** Overlapping steady-state activation (SSA) and inactivation (SSI) curves of average values (dots) and fitting to a Boltzmann equation (lines) for I_T in control-treated VB neurons recorded using 0.5 mM (filled dots) or 10 mM EGTA (empty dots) in the pipette solution. **e** Same as in plot (**d**) for "PACO"-like binge treated neurons represented in red. **f** and **g** Comparison of average V_{50} and k parameters from Boltzmann fitting corresponding to plots (**d**) and (**e**). *Significantly different ($p < 0.05$, ANOVA, see Table 2)

$Ca_v3.1$ (T-type, $\alpha 1G$ isoform) protein level was increased by sub-chronic administration of cocaine. In addition, we found a profound reduction of I_{H} density with the concomitant decrease of HCN2 mRNA level and a hyperpolarizing shift of

its steady-state activation curve. Therefore, in response to an inhibitory input, all these conditions generate a weak depolarizing force that would decrease the open probability of T-type Ca^{2+} channels, shaping LTS-associated Ca^{2+}

Table 2 Comparison of T-type current steady-state parameters of activation and inactivation in dialyzed neurons with either 0.5 or 10 mM EGTA for both control and “PACO” like binge treatments

EGTA concentration	Control		“PACO”-like binge		ANOVA <i>F</i> statistics
	0.5 mM	10 mM	0.5 mM	10 mM	
$V_{50 \text{ act.}}$ (mV)	-65.2 ± 1.5 (10)	-65 ± 1.7 (6)	-60.7 ± 1.7 (6)*	-67.5 ± 0.5 (7)	$F_{3,25} = 3.284$
$K_{\text{act.}}$ (mV)	2.3 ± 0.2 (10)	1.6 ± 0.3 (6)	4.0 ± 0.5 (6)*	1.8 ± 0.2 (7)	$F_{3,25} = 9.881$
$V_{50 \text{ inact.}}$ (mV)	-85.5 ± 1.4 (11)	-83.5 ± 0.6 (6)	-78.7 ± 1.0 (6)*	-87.4 ± 2 (7)	$F_{3,26} = 5.418$
$K_{\text{inact.}}$ (mV)	-5.3 ± 0.3 (11)	-6.3 ± 0.4 (6)	-5.6 ± 0.4 (6)	-6.1 ± 0.5 (7)	$F_{3,26} = 1.203$

Biophysical parameters (V_{50} and slope factor k) were obtained from the fit of activation and steady-state inactivation curves with the Boltzmann function. * $p < 0.05$, ANOVA

transients as observed in controls despite having an increased T-type current density. This effect was exclusively dependent on the combination of the psychostimulants; separately administration of cocaine or caffeine did not produce any effect on I_H .

Our results showed changes in the intrinsic properties of the VB neurons that persist after 24-h of a single (acute) or a chronic “PACO”-like binge consumption. We found that the input membrane resistance decreased after an acute binge, whereas it increased when the administration becomes chronic. Accordingly, we observed a binge-dependent regulation of I_H density, while it was increased by an acute binge, it was decreased by a chronic one. I_H -mediated alterations in membrane resistance will determine how the neurons respond to incoming stimulation (Magee 1998; Kase and Imoto 2012). We found that the membrane excitability decreased after an acute “PACO”-like binge administration, while it increased after a chronic administration. Furthermore, we observed alterations in the threshold of action potentials (APs). The increase of basal $[Ca^{2+}]_i$ in VB neurons 24-h after the systemic administration of an acute “PACO”-like binge might potentiate intracellular Ca^{2+} mediated inhibition of high-voltage-activated Ca^{2+} channels (Rankovic et al. 2010) and voltage-dependent Na^+ channels (Santarelli et al. 2007; Casini et al. 2009; Ulyanova and Shirokov 2018), blunting membrane depolarization mediated by these channels and decreasing the excitability of thalamocortical neurons, as we observed after an acute “PACO”-like binge. In addition, TREK K^+ channels are expressed in thalamocortical VB neurons (Meuth et al. 2006; Budde et al. 2008) and they have been described to influence the time-dependence of APs (Corbin-Leftwich et al. 2018). Caffeine has been reported to inhibit TREK-1 K^+ channels in a concentration- and cAMP-dependent manner (reviewed by Boison 2011).

Overall, our results showed that an acute “PACO”-like binge administration produced notorious alterations in the physiology of VB neurons, including enhancements of basal $[Ca^{2+}]_i$, upregulation of I_H density, and changes in biophysical properties of I_T that increased T-type “window currents.” As a

result, these alterations ultimately increased Ca^{2+} transients (LTS) associated to H and T-type currents and reduced the membrane excitability. Homeostatic mechanisms arise when the administration becomes chronic, such as downregulation of intracellular basal $[Ca^{2+}]_i$ to normal levels and reduction of I_H density, which not only reestablished the LTS-associated Ca^{2+} transients as observed in controls, but also increased the membrane excitability to values even higher than control.

Neuronal thalamocortical alterations contributed to sleep/wake transitions changes by chronic “PACO”-like binge treatments

Voltage-gated ionic channels have been extensively described to explain neuronal excitability, endowing them with auto rhythmic membrane oscillatory capabilities (Llinás 1988; 2005). Synaptic receptors mediate functional contacts between neurons, spreading oscillations throughout neuronal networks. In such networks, auto rhythmic neurons might either act as oscillators/pacemakers or as resonators (Llinás 1988; Llinás et al. 2005).

Coincidence detection by co-activation of the “specific” (i.e., VB relay thalamocortical neurons) and the “non-specific” (intralaminar) thalamic nuclei at gamma band frequencies has been proposed as the basis for the temporal conjunction that supports cognitive binding in the brain (Llinás et al. 2002). Abnormal low-frequency oscillatory activity of thalamocortical neurons, due to enhanced T-type calcium channel activation, has been related to altered thalamocortical dynamics described as the basis for several types of neurological and neuropsychiatric conditions, collectively named thalamocortical dysrhythmia syndrome (Llinás et al. 1999, 2005). “PACO”-like administrations described in this work mediated long-lasting, protracted activation of such low voltage activated (LVA) T-type calcium currents and altered I_H biophysics in VB thalamocortical neurons. These alterations could result in a thalamocortical stable dynamic attractor state of low-frequencies, that would be relayed from the thalamus to the cortical mantle (i.e., a dysrhythmic mechanism

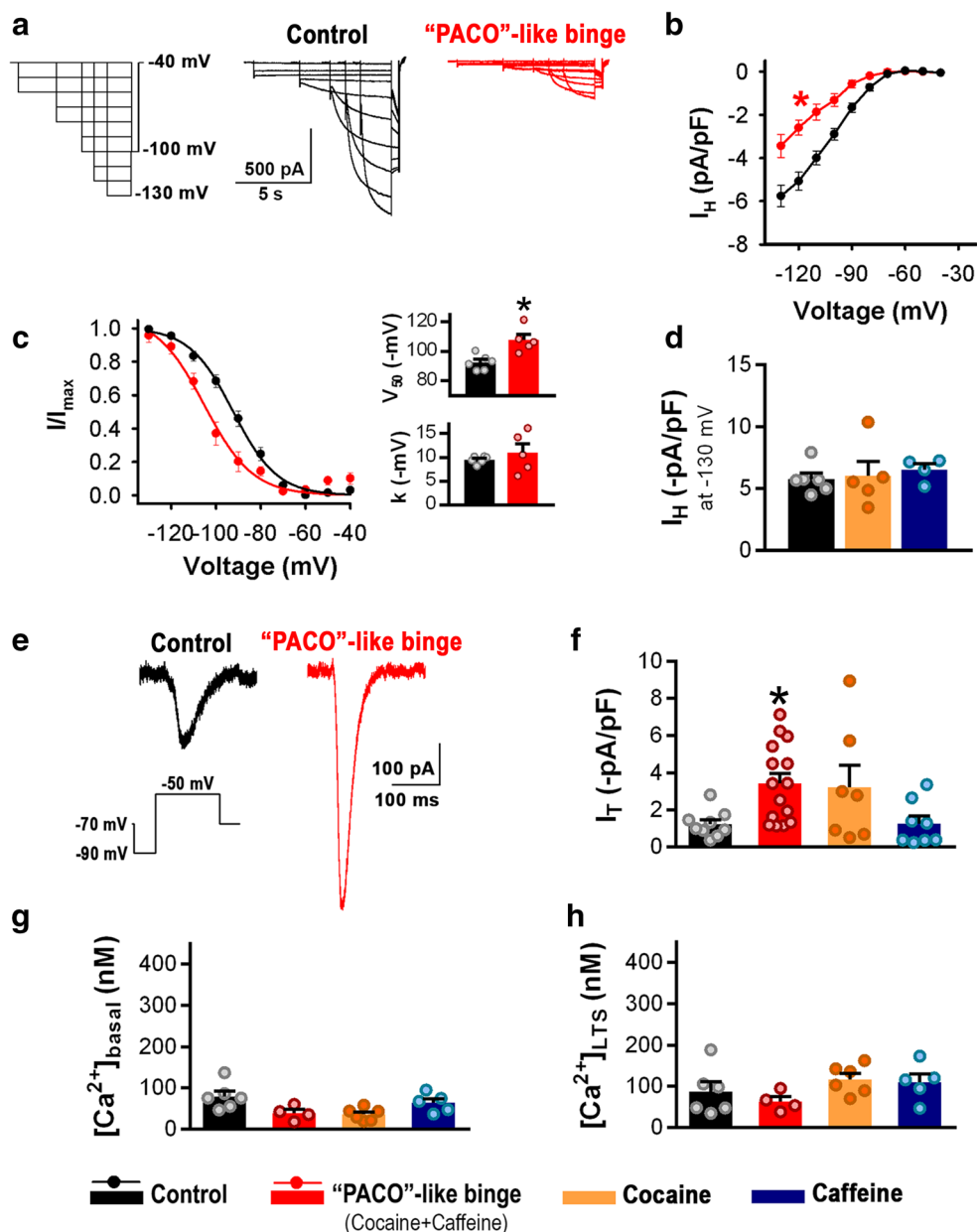


Fig. 6 Chronic “PACO”-like binge administration altered H current density in VB neurons. **a** Activation protocol (left plot) of HCN-mediated currents (I_H). Average traces of I_H , comparing VB neurons recorded from mice treated with a chronic “PACO”-like binge (red lines, right plot) and controls (black lines, middle plot). Note how “PACO”-like binge treated VB neurons presented less I_H . **b** Average I_H -voltage relationship (I-V curve) for control (black, $n = 6$) vs. “PACO”-like binge (red, $n = 5$) treatments. *Significantly different from control, $p < 0.001$. Two-way RM ANOVA, testing voltages (-90 to -130 mV, $F_{(4,36)} = 162.89$) and treatments ($F_{(1,36)} = 31.62$). There was a statistically significant interaction between the applied voltages and treatments ($F_{(4,36)} = 24.53$). **c** Steady-state activation (SSA) curves for control (black, $n = 6$) vs. “PACO”-like binge (red, $n = 5$) treatments. *Significantly different from control. Right bar plots representing average V_{50} and k , comparing control (black bar) and “PACO”-like binge (red bar). *Significantly different from control, $p < 0.01$. Student’s t test, $t_9 = 3.7$. **d** Bar plots comparing the

I_H density at -130 mV for controls ($n = 6$) and separately administration of cocaine ($n = 5$) or caffeine ($n = 4$) ($p > 0.05$, ANOVA). **e** Representative T-type Ca^{2+} current trace for control and “PACO”-like binge treatments. I_T was evoked by a voltage step from -90 to -50 mV. **f** Bar plots comparing the I_T density at -50 mV for controls ($n = 9$), “PACO”-like binge ($n = 15$) and separately administration of cocaine ($n = 7$) or caffeine ($n = 8$). *Significantly different from control and caffeine, $p < 0.05$, Kruskal-Wallis ANOVA on Ranks, $H_3 = 10.843$. Calcium imaging: **g** basal intracellular calcium concentration ($[Ca^{2+}]_{\text{basal}}$) (Mean \pm SEM) presented for control (black, $n = 6$), “PACO”-like (red, $n = 4$), cocaine (yellow, $n = 6$) and caffeine (blue, $n = 4$) treatments ($p > 0.05$, ANOVA). **h** LTS-associated Ca^{2+} transients ($[Ca^{2+}]_{\text{LTS}}$) (Mean \pm SEM) values are presented for control (black, $n = 6$), “PACO”-like (red, $n = 4$), cocaine (yellow, $n = 6$) and caffeine (blue, $n = 5$) treatments ($p > 0.05$, ANOVA)

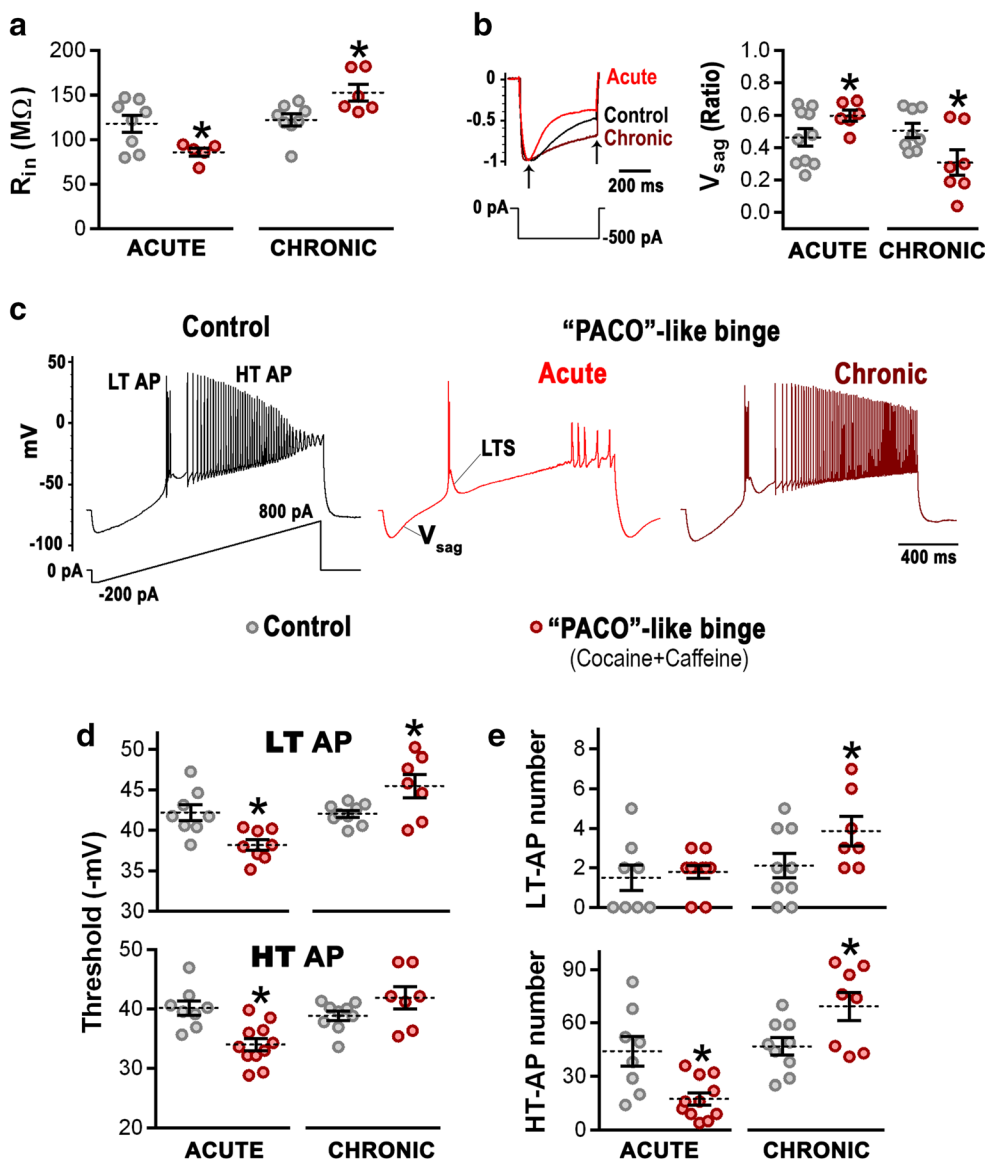
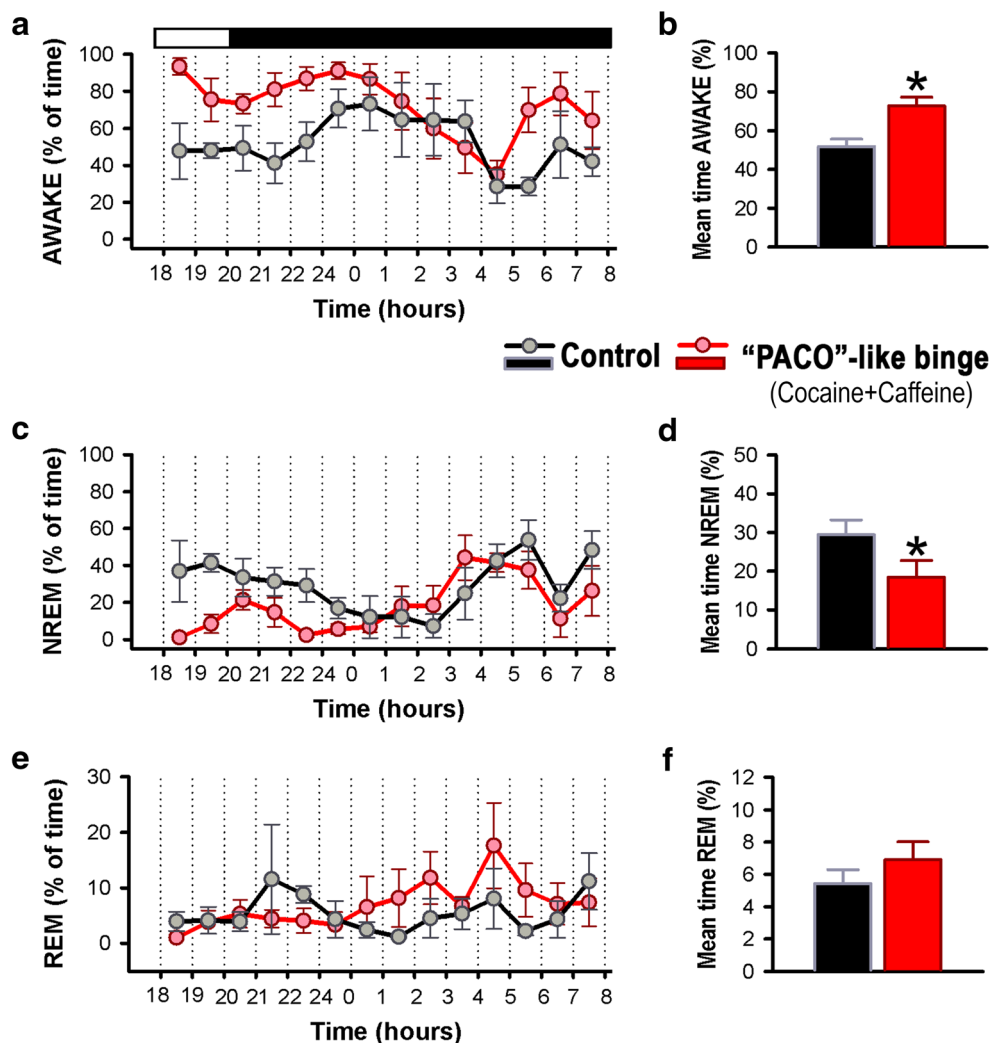


Fig. 7 Membrane excitability was altered 24-h after either acute or chronic “PACO”-like binge administration in VB neurons. **a** Input resistance (R_{in}) of VB neurons recorded after acute or chronic treatments, calculated as described in “Materials and Methods.” Left: scatter plots (Mean \pm SEM) comparing: control (black, $n = 8$) and “PACO”-like (red, $n = 5$) binges for acute treatments. $*p < 0.05$, Student’s t test, $t_{11} = 2.47$. Right: scatter plots (Mean \pm SEM) comparing: control (black, $n = 8$) and “PACO”-like (red, $n = 6$) binges for chronic treatments. $*p < 0.05$, Student’s t test, $t_{12} = -2.70$. **b** Left: average voltage traces of VB neurons recorded in current-clamp for control (black line), acute (red line) and chronic (maroon line) “PACO”-like binge treatments. Associated HCN-mediated currents induced voltage rectification (Voltage sag, V_{sag}), observed after a hyperpolarizing square pulse (-500 pA). Normalized traces are shown, see the small sag recorded after a chronic treatment. Right: voltage sag was calculated as $[(V_{peak} - V_{ss})/V_{peak}]$, where V_{peak} is the maximum instantaneous value (peak voltage) and V_{ss} the voltage reached at the steady state (see black arrows). Scatter plots (Mean \pm SEM) comparing acute ($n = 10$ for control and $n = 6$ for treated) and chronic ($n = 8$ for control and $n = 7$ for treated) binges versus control condition. $*p < 0.05$, Student’s t test, $t_{14} = -1.8$ for acute binges, $t_{13} = 2.28$ for chronic binges. **c** Representative current ramp stimulus (ramp rate of 0.67 pA/ms) applied after hyperpolarizing the membrane (-200 pA for 50 ms) to activate underlying H- and T-type channels for control (black line), acute (red line), or chronic (maroon line) “PACO”-like binges. Action potentials triggered by a

low-threshold spike (LTS) were called low-threshold action potentials (LT AP) and those triggered later were called high-threshold action potentials (HT AP). See the V_{sag} recorded after an acute “PACO”-like binge. **d** Top. Left: scatter plots (Mean \pm SEM) comparing the voltage threshold of LT AP for acute controls ($n = 8$) and “PACO”-like ($n = 8$) binges. $*p < 0.05$, Student’s t test, $t_{14} = 3.39$. Right: scatter plots (Mean \pm SEM) comparing the voltage threshold of LT AP for chronic controls ($n = 9$) and “PACO”-like ($n = 7$) binges. $*p < 0.05$, Student’s t test, $t_{14} = -2.52$. Bottom. Left: Scatter plots (Mean \pm SEM) comparing the voltage threshold of HT AP for acute controls ($n = 8$) and “PACO”-like ($n = 8$) binges. $*p < 0.05$, Student’s t test, $t_{17} = 3.83$. Right: scatter plots (Mean \pm SEM) comparing the voltage threshold of HT AP for chronic controls ($n = 9$) and “PACO”-like ($n = 7$) binges ($p > 0.05$, Mann-Whitney Rank Sum Test). **e** Top. Left: scatter plots (Mean \pm SEM) comparing the number of LT AP for acute controls ($n = 8$) and “PACO”-like ($n = 10$) binges ($p > 0.05$, Mann-Whitney Rank Sum Test). Right: scatter plots (Mean \pm SEM) comparing the number of LT AP for chronic controls ($n = 9$) and “PACO”-like ($n = 7$) binges. $*p < 0.05$, Student’s t test, $t_{14} = -1.84$. Bottom. Left: scatter plots (Mean \pm SEM) comparing the number of HT AP for acute controls ($n = 8$) and “PACO”-like ($n = 11$) binges. $*p < 0.05$, Student’s t test, $t_{17} = 3.28$. Right: scatter plots (Mean \pm SEM) comparing the number of HT AP for chronic controls ($n = 9$) and “PACO”-like ($n = 8$) binges. $*p < 0.05$, Student’s t test, $t_{15} = -2.48$

Fig. 8 Effects of chronic binge treatments on awake, NREM and REM sleep phases during electroencephalography recordings in mice. **a** Mean percentage of time in the awake stage plotted for every hour of 14-h recordings the transition from 18 h of the previous day until 8 h of the next day comparing mice 24 h after chronically treated with a “PACO”-like binge (red circles) versus vehicle (saline, black circles). Note that upper bar represents light (empty bar)/dark (filled bar) status during recordings. **b** Mean total awake time from cocaine+caffeine (red bar) and saline (black bar). *Significantly different from saline (Student’s *t* test; $t = 4.5$; $p < 0.001$). **c** and **d** Same for NREM sleep. *Significantly different from saline (Student’s *t* test, $df = 13$; $t = 2.6$; $p < 0.05$). **e** and **f** Same for REM sleep



originated in a ‘bottom-up’ fashion). On the other hand, robust low-frequency and high-frequency interaction between nearby cortical columns generates asymmetric cortical inhibition called the edge-effect, a condition akin to a cortical correlation of thalamocortical dysrhythmia syndrome originated in a “top-down” fashion (Llinás et al. 2005). This contrast between “PACO”-like mediated mismatched inputs to the cortex is thought to produce alterations of sensory inputs processing as well as abrupt changes in sleep/wake transitions in the EEG. These mechanisms might result in long-lasting, potentially permanent changes in thalamocortical-cortical processing.

Thalamocortical and striatal-cortical neurons have been described to be robustly interconnected (Albin et al. 1989). Both thalamocortical and striatal neurons have been described to be modulated by extracellular, synaptic monoaminergic augmentation mediated by cocaine (Urbano et al. 2015; Bisagno et al. 2016; Urbano and Bisagno 2017). We have previously described that “PACO”-like binge increased hyperlocomotion (Muñiz et al. 2016) and altered the expression of genes

involved in glutamatergic and dopaminergic neurotransmission in the mesolimbic reward system (Muñiz et al. 2017). Furthermore, both caffeine and serotonin receptors have been described to modulate VB neurons (Goitia et al. 2016).

T-type and HCN channels are physically and functionally associated (Huang et al. 2011; Fan et al. 2017) to underlie low-frequency oscillatory activity at the thalamocortical level that can be characterized using electroencephalography (EEG) (Llinás et al. 2007; Urbano et al. 2009; Huang et al. 2011). Indeed, T-type channels have been described as key elements involved in the sensitivity to psychostimulants (Bisagno et al. 2010; Goitia et al. 2013, 2016; Gangarossa et al. 2014). On the other hand, the amplitude of I_H can be increased in the presence of a calcium-dependent increase in intracellular cAMP mediated by monoamine receptors such as norepinephrine and serotonin (Lüthi and McCormick 1999; Frère and Lüthi 2004), which causes failure to maintain the oscillatory trigger mode (Yue 2001). Dysregulation of I_H has been linked to several neurological disorders with concomitant changes in thalamocortical/corticothalamic oscillatory activities such as

in certain types of epilepsy (Cain et al. 2015; Zobeiri et al. 2018). After an acute administration of a “PACO”-like binge, the increase of I_H density and the rightward shift of the steady-state properties of T-type channels will depolarize the threshold potential between the two firing modalities of VB neurons to values close to their resting potential. Therefore, VB neurons will be in transition between their firing modalities: oscillatory during slow (NREM) sleep and tonic during wakefulness and REM sleep. However, when the administration becomes chronic, VB neurons displayed a pronounced reduction of I_H density, resulting in an increased input resistance that will alter the response to depolarizing inputs and the susceptibility for oscillations. The density and properties of I_H are crucial factors in the generation and termination of sleep-related thalamocortical activity (Kanyshkova et al. 2009). Since I_H was sharply decreased 24-h after a chronic “PACO”-like binge administration, we were interested in a further characterization using EEG. We observed alterations of wake/sleep transitions, the awake percentage of time was increased and the NREM sleep percentage of time was decreased after chronic “PACO”-like binge treatment, in accordance with the observed reduction of I_H (Kanyshkova et al. 2009). Results presented here are consistent with a recent report showing increased time in the awake stage of rats 2 days after i.p. administration of “coca paste” adulterated with caffeine (Schwarzkopf et al. 2018). EEG recordings in rats have shown a decrease in the “power spectrum” of NREM sleep after a daily systemic (i.p.) administration of cocaine hydrochloride (15 mg/kg) (Binienda et al. 2006). In mice, when cocaine is administered systemically (i.p.), acute “binge” scheme significantly increased both I_H and I_T densities and NREM sleep low frequency oscillations, without changes in high frequencies (Urbano et al. 2009). In humans, cocaine administration suppresses REM sleep with subsequent rebound (that is, it increases the time in REM and decreases the latency to enter REM sleep [Morgan et al. 2008]). Withdrawal after chronic cocaine consumption altered sleep cytoarchitecture in patients who used cocaine (Angarita et al. 2014).

Sleep problems have been associated with the use of stimulants. Almost 70% of patients admitted for detoxification report sleep problems before admission, and 80% of those who report sleep problems are related to cocaine use, among others (Roncero et al. 2012). Alterations in the organization of sleep stages increased the risk of developing drug abuse disorders, and also chronic consumption of drugs of abuse lead to chronic sleep problems and diseases (Budney et al. 2003; Burke et al. 2008).

Further studies are needed in order to better characterize the role of cortical areas on the alterations observed here after combined cocaine and caffeine administration. Furthermore, unbalanced synaptic interactions between thalamocortical

neurons after psychostimulant administration need further study.

Limitations and future perspectives

The characterization of the functional alterations in the somatosensory thalamocortical system of animals exposed to cocaine and caffeine could contribute to the characterization of the harmful effects of these drugs, expanding the field of knowledge in the area of Neurobiology of drugs of abuse. Even though Argentina suffers from serious public health problems related to drugs of abuse and in particular the “PACO,” the number of research groups that study these issues is small. More data comparing the effects of illegally consumed “PACO” samples obtained by South American judiciary branch with results described here is key. Future experiments are still needed in order to explore the possible role of membrane channels in charge of finely tune membrane potential (e.g., K_2P , HCN, leak channels) on “PACO”-mediated thalamocortical deleterious effects.

Conclusions

Our results showed changes in the intrinsic properties of the ventrobasal nucleus neurons 24-h after either acute or chronic binge administrations of combined cocaine and caffeine (“PACO”-like binge). Acute treatments increased H-current density mediated by HCN channels and enhanced basal $[Ca^{2+}]_i$ that modulated biophysical properties of T-type Ca^{2+} channels. These alterations ultimately increased LTS-associated Ca^{2+} transients and reduced the membrane excitability of ventrobasal neurons. Chronic treatments exhibited a downregulation of basal $[Ca^{2+}]_i$ and a reduction of I_H density, which not only reestablished the LTS-associated Ca^{2+} transients as observed in controls, but also increased the membrane excitability. Chronic treatments were capable of not only altering intrinsic properties of thalamocortical neurons but also increasing awake percentage while reducing NREM sleep time during electroencephalography recordings.

Acknowledgments The authors would like remember our recently deceased colleague Dr. Carlota Gonzalez-Inchauspe. Carlota has been a brilliant and hardworking neuroscientist that has been working with us for a long time. Her experiments and data analysis made possible this paper. In the middle of the COVID-19 pandemic, Carlota has passed away last June 2020 just weeks away prior submission of this manuscript. In addition, the authors would like to thank Dr. Javier Muñoz and Maria Emilia Ferro for their help during initial setup of our electroencephalography rig. This work was supported by grants from FONCYT-Agencia Nacional de Promoción Científica y Tecnológica; Préstamo BID 1728 OC.AR.PICT [Grant numbers: 2016-1728 and 2018-1744]; and Argentina-Germany collaboration grant, CONICET-DFG-MINCYT [Grant number: 2016-23120160100012CO01] to Dr. Urbano. FONCYT-Agencia Nacional de Promoción Científica y Tecnológica;

Préstamo BID 1728 OC.AR.PICT [Grant numbers: 2012-0924 and 2015-2594] to Dr. Bisagno. FONCYT-Agencia Nacional de Promoción Científica y Tecnológica; Préstamo BID 1728 OC.AR.PICT [Grant number: 2016-1799] to Dr. Perissinotti.

Authors' contributions Maria Celeste Rivero-Echeto: methodology, investigation, formal analysis, writing—review & editing. Paula P. Perissinotti: methodology, investigation, formal analysis, writing—original draft. Carlota Gonzalez-Inchauspe: methodology, investigation & formal analysis. Lucila Kargieman: formal analysis, writing—review & editing. Veronica Bisagno: methodology, investigation, resources, supervision, funding acquisition, writing - review & editing. Francisco J. Urbano: methodology, investigation, resources, supervision, project administration, funding acquisition, writing—original draft.

Funding This work was supported by grants from FONCYT-Agencia Nacional de Promoción Científica y Tecnológica; Préstamo BID 1728 OC.AR.PICT [Grant numbers: 2016-1728 and 2018-1744]; and Argentina-Germany collaboration grant, CONICET-DFG-MINCYT [Grant number: 2016-23120160100012CO01] to Dr. Urbano. FONCYT-Agencia Nacional de Promoción Científica y Tecnológica; Préstamo BID 1728 OC.AR.PICT [Grant numbers: 2012-0924 and 2015-2594] to Dr. Bisagno. FONCYT-Agencia Nacional de Promoción Científica y Tecnológica; Préstamo BID 1728 OC.AR.PICT [Grant number: 2016-1799] to Dr. Perissinotti.

Compliance with ethical standards

Research involving human participants and/or animals This article does not contain any studies with human participants performed by any of the authors. All procedures performed in studies involving animals (mice) were in accordance with the ethical standards of the Central Animal Facility at the University of Buenos Aires (animal protocol #50-2015, and #67-2015). Principles of mice care of the Central Animal Facility (University of Buenos Aires) were in accordance with the National Institutes of Health guide (NIH Publications, No. 8023, revised 1978) for the care and use of Laboratory animals, ARRIVE guidelines and CONICET (2003), and approved by its authorities using OLAW/ARENA directives (NIH, Bethesda, MD, USA). The experiments in this study complied with the current laws of Argentina. Authors have full control of all primary data and agree to allow the journal to review their data if requested.

Conflict of interest The authors declare that they have no conflict of interest.

References

- Albin RL, Young AB, Penney JB (1989) The functional anatomy of basal ganglia disorders. *Trends Neurosci* 12(10):366–375. [https://doi.org/10.1016/0166-2236\(89\)90074-x](https://doi.org/10.1016/0166-2236(89)90074-x)
- Angarita GA, Canavan SV, Forselius E, Bessette A, Morgan PT (2014) Correlates of polysomnographic sleep changes in cocaine dependence: self-administration and clinical outcomes. *Drug Alcohol Depend* 143:173–180. <https://doi.org/10.1016/j.drugalcdep.2014.07.025>
- Aoyama K, Matsumura N, Watabe M, Wang F, Kikuchi-Utsumi K, Nakaki T (2011) Caffeine and uric acid mediate glutathione synthesis for neuroprotection. *Neuroscience* 181:206–215. <https://doi.org/10.1016/j.neuroscience.2011.02.047>
- Asmara H, Micu I, Rizwan AP, Sahu G, Simms BA, Zhang FX, Engbers JDT, Stys PK, Zamponi GW, Tumer RW (2017) A T-type channel-calmodulin complex triggers α CaMKII activation. *Mol Brain* 10(1):37. <https://doi.org/10.1186/s13041-017-0317-8>
- Behrendt R-P (2006) Dysregulation of thalamic sensory ‘transmission’ in schizophrenia: neurochemical vulnerability to hallucinations. *J Psychopharmacol* 20:356–372. <https://doi.org/10.1177/0269881105057696>
- Bijlenga P, Liu J-H, Espinos E, Haenggeli CA, Fischer-Lougheed J, Bader CR, Bernheim L (2000) T-type α 1H Ca²⁺ channels are involved in Ca²⁺ signaling during terminal differentiation (fusion) of human myoblasts. *Proc Natl Acad Sci* 97:7627–7632. <https://doi.org/10.1073/pnas.97.13.7627>
- Binienda ZK, Pereira F, Alper K et al (2006) Adaptation to repeated cocaine administration in rats. *Ann N Y Acad Sci* 965:172–179. <https://doi.org/10.1111/j.1749-6632.2002.tb04159.x>
- Bisagno V, Raineri M, Peskin V, Wikinski SI, Uchitel OD, Llinás RR, Urbano FJ (2010) Effects of T-type calcium channel blockers on cocaine-induced hyperlocomotion and thalamocortical GABAergic abnormalities in mice. *Psychopharmacology* 212:205–214. <https://doi.org/10.1007/s00213-010-1947-z>
- Bisagno V, González B, Urbano FJ (2016) Cognitive enhancers versus addictive psychostimulants: the good and bad side of dopamine on prefrontal cortical circuits. *Pharmacol Res* 109:108–118. <https://doi.org/10.1016/j.phrs.2016.01.013>
- Boison D (2011) Methylxanthines, seizures, and excitotoxicity. In: *Methylxanthines*. Springer, Berlin Heidelberg, Berlin, Heidelberg, pp 251–266. https://doi.org/10.1007/978-3-642-13443-2_9
- Brennan GP, Baram TZ, Poolos NP (2016) Hyperpolarization-activated cyclic nucleotide-gated (HCN) channels in epilepsy. *Cold Spring Harb Perspect Med* 6:a022384. <https://doi.org/10.1101/cshperspect.a022384>
- Budde T, Coulon P, Pawlowski M, Meuth P, Kanyshkova T, Japes A, Meuth SG, Pape HC (2008) Reciprocal modulation of I_h and I_{TASK} in thalamocortical relay neurons by halothane. *Pflugers Arch - Eur J Physiol* 456:1061–1073. <https://doi.org/10.1007/s00424-008-0482-9>
- Budney AJ, Moore BA, Vandrey RG, Hughes JR (2003) The time course and significance of cannabis withdrawal. *J Abnorm Psychol* 112:393–402. <https://doi.org/10.1037/0021-843X.112.3.393>
- Burke CK, Peirce JM, Kidorf MS, Neubauer D, Punjabi NM, Stoller KB, Hursh S, Brooner RK (2008) Sleep problems reported by patients entering opioid agonist treatment. *J Sub Abuse Treat* 35:328–333. <https://doi.org/10.1016/j.jsat.2007.10.003>
- Cadet JL, Bisagno V (2013) The primacy of cognition in the manifestations of substance use disorders. *Front Neurol* 4. <https://doi.org/10.3389/fneur.2013.00189>
- Cadet JL, Bisagno V, Milroy CM (2014) Neuropathology of substance use disorders. *Acta Neuropathol* 127:91–107. <https://doi.org/10.1007/s00401-013-1221-7>
- Cain SM, Tyson JR, Jones KL, Snutch TP (2015) Thalamocortical neurons display suppressed burst-firing due to an enhanced I_h current in a genetic model of absence epilepsy. *Pflugers Arch - Eur J Physiol* 467:1367–1382. <https://doi.org/10.1007/s00424-014-1549-4>
- Casini S, Verkerk AO, van Borren MMGJ, van Ginneken ACG, Veldkamp MW, de Bakker JMT, Tan HL (2009) Intracellular calcium modulation of voltage-gated sodium channels in ventricular myocytes. *Cardiovasc Res* 81:72–81. <https://doi.org/10.1093/cvr/cvn274>
- Cazade M, Bidaud I, Lory P, Chemin J (2017) Activity-dependent regulation of T-type calcium channels by submembrane calcium ions. *eLife* 6:e22331. <https://doi.org/10.7554/eLife.22331>
- Corbin-Leftwich A, Small HE, Robinson HH, Villalba-Galea CA, Boland LM (2018) A xenopus oocyte model system to study action potentials. *J Gen Physiol* 150:1583–1593. <https://doi.org/10.1085/jgp.201812146>
- Coulon P, Herr D, Kanyshkova T, Meuth P, Budde T, Pape HC (2009) Burst discharges in neurons of the thalamic reticular nucleus are

- shaped by calcium-induced calcium release. *Cell Calcium* 46:333–346. <https://doi.org/10.1016/j.ceca.2009.09.005>
- Crunelli V, Tóth TI, Cope DW, Blethyn K, Hughes SW (2005) The ‘window’ T-type calcium current in brain dynamics of different behavioural states: neuronal $I_{T\text{window}}$. *J Physiol* 562:121–129. <https://doi.org/10.1113/jphysiol.2004.076273>
- Deisseroth K, Bitó H, Tsien RW (1996) Signaling from synapse to nucleus: postsynaptic CREB phosphorylation during multiple forms of hippocampal synaptic plasticity. *Neuron* 16:89–101. [https://doi.org/10.1016/S0896-6273\(00\)80026-4](https://doi.org/10.1016/S0896-6273(00)80026-4)
- Devlin RJ, Henry JA (2008) Clinical review: major consequences of illicit drug consumption. *Crit Care* 12:202. <https://doi.org/10.1186/cc6166>
- Di Guilmi MN, Wang T, Inchauspe CG et al (2014) Synaptic gain-of-function effects of mutant Cav2.1 channels in a mouse model of familial hemiplegic migraine are due to increased basal $[Ca^{2+}]_i$. *J Neurosci* 34:7047–7058. <https://doi.org/10.1523/JNEUROSCI.2526-13.2014>
- Du C, Yu M, Volkow ND et al (2006) Cocaine increases the intracellular calcium concentration in brain independently of its cerebrovascular effects. *J Neurosci* 26:11522–11531. <https://doi.org/10.1523/JNEUROSCI.3612-06.2006>
- Fan J, Gandini MA, Zhang F-X, Chen L, Souza IA, Zamponi GW (2017) Down-regulation of T-type Cav3.2 channels by hyperpolarization-activated cyclic nucleotide-gated channel 1 (HCN1): evidence of a signaling complex. *Channels* 11:434–443. <https://doi.org/10.1080/19336950.2017.1326233>
- Fontanez DE, Porter JT (2006) Adenosine A1 receptors decrease thalamic excitation of inhibitory and excitatory neurons in the barrel cortex. *Neuroscience* 137:1177–1184. <https://doi.org/10.1016/j.neuroscience.2005.10.022>
- Fredholm BB (1995) Adenosine, adenosine receptors and the actions of caffeine. *Pharmacol Toxicol* 76:93–101. <https://doi.org/10.1111/j.1600-0773.1995.tb00111.x>
- Fredholm BB, Bättig K, Holmén J, Nehlig A, Zvartau EE (1999) Actions of caffeine in the brain with special reference to factors that contribute to its widespread use. *Pharmacol Rev* 51:83–133
- Frère SGA, Lüthi A (2004) Pacemaker channels in mouse thalamocortical neurones are regulated by distinct pathways of cAMP synthesis: cAMP signalling in thalamocortical neurones. *J Physiol* 554:111–125. <https://doi.org/10.1113/jphysiol.2003.050989>
- Gangarossa G, Laffray S, Bourinet E, Valjent E (2014) T-type calcium channel Cav3.2 deficient mice show elevated anxiety, impaired memory and reduced sensitivity to psychostimulants. *Front Behav Neurosci* 8. <https://doi.org/10.3389/fnbeh.2014.00092>
- Garaschuk O, Yaari Y, Konnerth A (1997) Release and sequestration of calcium by ryanodine-sensitive stores in rat hippocampal neurones. *J Physiol* 502:13–30. <https://doi.org/10.1111/j.1469-7793.1997.013bl.x>
- Goitia B, Raineri M, González LE, Rozas JL, Garcia-Rill E, Bisagno V, Urbano FJ (2013) Differential effects of methylphenidate and cocaine on GABA transmission in sensory thalamic nuclei. *J Neurochem* 124:602–612. <https://doi.org/10.1111/jnc.12113>
- Goitia B, Rivero-Echeto MC, Weisstaub NV, Gingrich JA, Garcia-Rill E, Bisagno V, Urbano FJ (2016) Modulation of GABA release from the thalamic reticular nucleus by cocaine and caffeine: role of serotonin receptors. *J Neurochem* 136:526–535. <https://doi.org/10.1111/jnc.13398>
- Hanson GR, Jensen M, Johnson M, White HS (1999) Distinct features of seizures induced by cocaine and amphetamine analogs. *Eur J Pharmacol* 377:167–173. [https://doi.org/10.1016/S0014-2999\(99\)00419-7](https://doi.org/10.1016/S0014-2999(99)00419-7)
- Heppert K, Davies M (1999) Simultaneous determination of caffeine from blood, brain and muscle using microdialysis in an awake rat and the effect of caffeine on rat activity. *Curr Sep* 18:3–8
- Huang Z-L, Urade Y, Hayaishi O (2011) The role of adenosine in the regulation of sleep. *CTMC* 11:1047–1057. <https://doi.org/10.2174/156802611795347654>
- Hughes SW, Cope DW, Tóth TI, Williams SR, Crunelli V (1999) All thalamocortical neurones possess a T-type Ca^{2+} ‘window’ current that enables the expression of bistability-mediated activities. *J Physiol* 517:805–815. <https://doi.org/10.1111/j.1469-7793.1999.0805s.x>
- Jahnsen H, Llinás R (1984a) Ionic basis for the electro-responsiveness and oscillatory properties of guinea-pig thalamic neurones in vitro. *J Physiol* 349:227–247. <https://doi.org/10.1113/jphysiol.1984.sp015154>
- Jahnsen H, Llinás R (1984b) Electrophysiological properties of guinea-pig thalamic neurones: an in vitro study. *J Physiol* 349:205–226. <https://doi.org/10.1113/jphysiol.1984.sp015153>
- Kanyshkova T, Pawlowski M, Meuth P, Dube C, Bender RA, Brewster AL, Baumann A, Baram TZ, Pape HC, Budde T (2009) Postnatal expression pattern of HCN channel isoforms in thalamic neurons: relationship to maturation of thalamocortical oscillations. *J Neurosci* 29:8847–8857. <https://doi.org/10.1523/JNEUROSCI.0689-09.2009>
- Kase D, Imoto K (2012) The role of HCN channels on membrane excitability in the nervous system. *J Signal Transduc* 2012:1–11. <https://doi.org/10.1155/2012/619747>
- Lambert RC, Bessaih T, Crunelli V, Leresche N (2014) The many faces of T-type calcium channels. *Pflugers Arch - Eur J Physiol* 466:415–423. <https://doi.org/10.1007/s00424-013-1353-6>
- Lazarus M, Shen H-Y, Cherasse Y, Qu WM, Huang ZL, Bass CE, Winsky-Sommerer R, Semba K, Fredholm BB, Boison D, Hayaishi O, Urade Y, Chen JF (2011) Arousal effect of caffeine depends on adenosine A2A receptors in the shell of the nucleus accumbens. *J Neurosci* 31:10067–10075. <https://doi.org/10.1523/JNEUROSCI.6730-10.2011>
- Llinás R (1988) The intrinsic electrophysiological properties of mammalian neurons: insights into central nervous system function. *Science* 242:1654–1664. <https://doi.org/10.1126/science.3059497>
- Llinás R, Leznik E, Urbano FJ (2002) Temporal binding via cortical coincidence detection of specific and nonspecific thalamocortical inputs: A voltage-dependent dye-imaging study in mouse brain slices. *Proceedings of the National Academy of Sciences* 99(1): 449–454. <https://doi.org/10.1073/pnas.012604899>
- Llinás R, Urbano FJ, Leznik E, Ramírez RR, van Marle HJF (2005) Rhythmic and dysrhythmic thalamocortical dynamics: GABA systems and the edge effect. *Trends Neurosci* 28:325–333. <https://doi.org/10.1016/j.tins.2005.04.006>
- Llinás RR, Ribary U, Jeanmonod D, Kronberg E, Mitra PP (1999) Thalamocortical dysrhythmia: A neurological and neuropsychiatric syndrome characterized by magnetoencephalography. *Proceedings of the National Academy of Sciences* 96:15222–15227. <https://doi.org/10.1073/pnas.96.26.15222>
- Llinás RR, Choi S, Urbano FJ, Shin H-S (2007) Band deficiency and abnormal thalamocortical activity in P/Q-type channel mutant mice. *Proc Natl Acad Sci U S A* 104:17819–17824. <https://doi.org/10.1073/pnas.0707945104>
- López-Hill X, Prieto JP, Meikle MN, Urbanavicius J, Abin-Carriquiry JA, Prunell G, Umpiérrez E, Scorza MC (2011) Coca-paste seized samples characterization: chemical analysis, stimulating effect in rats and relevance of caffeine as a major adulterant. *Behav Brain Res* 221:134–141. <https://doi.org/10.1016/j.bbr.2011.03.005>
- López-Rodríguez AB, Viveros M-P (2019) Bath salts and polyconsumption: in search of drug-drug interactions. *Psychopharmacology* 236:1001–1014. <https://doi.org/10.1007/s00213-019-05213-3>
- Lüthi A, McCormick DA (1999) Modulation of a pacemaker current through Ca^{2+} -induced stimulation of cAMP production. *Nat Neurosci* 2:634–641. <https://doi.org/10.1038/10189>

- Lüthi A, Bal T, McCormick DA (1998) Periodicity of thalamic spindle waves is abolished by ZD7288, a blocker of I_h . *J Neurophysiol* 79: 3284–3289. <https://doi.org/10.1152/jn.1998.79.6.3284>
- Magee JC (1998) Dendritic hyperpolarization-activated currents modify the integrative properties of hippocampal CA1 pyramidal neurons. *J Neurosci* 18:7613–7624. <https://doi.org/10.1523/JNEUROSCI.18-19-07613.1998>
- Marty A, Neher E (1985) Potassium channels in cultured bovine adrenal chromaffin cells. *J Physiol* 367:117–141. <https://doi.org/10.1113/jphysiol.1985.sp015817>
- Meuth SG, Kanyshkova T, Meuth P, Landgraf P, Munsch T, Ludwig A, Hofmann F, Pape HC, Budde T (2006) Membrane resting potential of thalamocortical relay neurons is shaped by the interaction among TASK3 and HCN2 channels. *J Neurophysiol* 96:1517–1529. <https://doi.org/10.1152/jn.01212.2005>
- Momin A, Cadiou H, Mason A, McNaughton PA (2008) Role of the hyperpolarization-activated current I_h in somatosensory neurons: role of I_h in nociception. *J Physiol* 586:5911–5929. <https://doi.org/10.1113/jphysiol.2008.163154>
- Morgan PT, Pace-Schott EF, Sahul ZH, Coric V, Stickgold R, Malison RT (2008) Sleep architecture, cocaine and visual learning. *Addiction* 103:1344–1352. <https://doi.org/10.1111/j.1360-0443.2008.02233.x>
- Muñiz JA, Gomez G, González B, Rivero-Echeto MC, Cadet JL, García-Rill E, Urbano FJ, Bisagno V (2016) Combined effects of simultaneous exposure to caffeine and cocaine in the mouse striatum. *Neurotox Res* 29:525–538. <https://doi.org/10.1007/s12640-016-9601-0>
- Muñiz JA, Prieto JP, González B, Sosa MH, Cadet JL, Scorza C, Urbano FJ, Bisagno V (2017) Cocaine and caffeine effects on the conditioned place preference test: concomitant changes on early genes within the mouse prefrontal cortex and nucleus Accumbens. *Front Behav Neurosci* 11:200. <https://doi.org/10.3389/fnbeh.2017.00200>
- Perissinotti PP, Ethington EG, Cribbs L, Koob MD, Martin J, Piedras-Rentería ES (2014) Down-regulation of endogenous KLHL1 decreases voltage-gated calcium current density. *Cell Calcium* 55: 269–280. <https://doi.org/10.1016/j.ceca.2014.03.002>
- Perissinotti PP, Rivero-Echeto MC, Garcia-Rill E, Bisagno V, Urbano FJ (2018) Leptin alters somatosensory thalamic networks by decreasing gaba release from reticular thalamic nucleus and action potential frequency at ventrobasal neurons. *Brain Struct Funct* 223:2499–2514. <https://doi.org/10.1007/s00429-018-1645-x>
- Prieto JP, Scorza C, Serra GP, Perra V, Galvalisi M, Abin-Carriquiry JA, Piras G, Valentini V (2016) Caffeine, a common active adulterant of cocaine, enhances the reinforcing effect of cocaine and its motivational value. *Psychopharmacology* 233:2879–2889. <https://doi.org/10.1007/s00213-016-4320-z>
- Prieto JP, González B, Muñiz J, Bisagno V, Scorza C (2020) Molecular changes in the nucleus accumbens and prefrontal cortex associated with the locomotor sensitization induced by coca paste seized samples. *Psychopharmacology* 237:1481–1491. <https://doi.org/10.1007/s00213-020-05474-3>
- Rankovic V, Ehling P, Coulon P, Landgraf P, Kreutz MR, Munsch T, Budde T (2010) Intracellular Ca^{2+} release-dependent inactivation of Ca^{2+} currents in thalamocortical relay neurons. *Eur J Neurosci* 31: 439–449. <https://doi.org/10.1111/j.1460-9568.2010.07081.x>
- Richter TA (2005) Low voltage-activated Ca^{2+} channels are coupled to Ca^{2+} -induced Ca^{2+} release in rat thalamic midline neurons. *J Neurosci* 25:8267–8271. <https://doi.org/10.1523/JNEUROSCI.1942-05.2005>
- Roberts WM (1993) Spatial calcium buffering in saccular hair cells. *Nature* 363:74–76. <https://doi.org/10.1038/363074a0>
- Roncero C, Grau-López L, Diaz-Morán S, Miquel L, Martínez-Luna N, Casas M (2012) Evaluation of sleep disorders in drug dependent inpatients (in spanish). *Med Clin* 138:332–335. <https://doi.org/10.1016/j.medcli.2011.07.015>
- Rozas JL, Goitia B, Bisagno V, Urbano FJ (2017) Differential alterations of intracellular $[Ca^{2+}]$ dynamics induced by cocaine and methylphenidate in thalamocortical ventrobasal neurons. *Transl Brain Rhythmicity* 2. <https://doi.org/10.15761/TBR.1000114>
- Santarelli VP, Eastwood AL, Dougherty DA, Horn R, Ahern CA (2007) A cation- interaction discriminates among sodium channels that are either sensitive or resistant to Tetrodotoxin block. *J Biol Chem* 282: 8044–8051. <https://doi.org/10.1074/jbc.M611334200>
- Schwarzkopf N, Lagos P, Falconi A, Scorza C, Torterolo P (2018) Caffeine as an adulterant of coca paste seized samples: preclinical study on the rat sleep–wake cycle. *Behav Pharmacol* 29:519–529. <https://doi.org/10.1097/FBP.0000000000000417>
- Steriade M, Amzica F (1996) Intracortical and corticothalamic coherency of fast spontaneous oscillations. *Proc Natl Acad Sci U S A* 93:2533–2538. <https://doi.org/10.1073/pnas.93.6.2533>
- Ulyanova AV, Shirokov RE (2018) Voltage-dependent inward currents in smooth muscle cells of skeletal muscle arterioles. *PLoS One* 13: e0194980. <https://doi.org/10.1371/journal.pone.0194980>
- Urbano FJ, Bisagno V (2017) Cocaine enhances gamma-aminobutyric acid release from reticular thalamic nucleus. In: *The Neuroscience of Cocaine*. Elsevier, pp. 511–518
- Urbano FJ, Bisagno V, Wikinski SI, Uchitel OD, Llinás RR (2009) Cocaine acute “binge” administration results in altered thalamocortical interactions in mice. *Biol Psychiatry* 66:769–776. <https://doi.org/10.1016/j.biopsych.2009.04.026>
- Urbano FJ, Bisagno V, González B, Celeste Rivero-Echeto M, Muñiz JA, Luster B, D’Onofrio S, Mahaffey S, Garcia-Rill E (2015) Pedunculopontine arousal system physiology—effects of psychostimulant abuse. *Sleep Sci* 8:162–168. <https://doi.org/10.1016/j.slsci.2015.09.004>
- Usachev Y, Shmigol A, Pronchuk N, Kostyuk P, Verkhratsky A (1993) Caffeine-induced calcium release from internal stores in cultured rat sensory neurons. *Neuroscience* 57:845–859. [https://doi.org/10.1016/0306-4522\(93\)90029-F](https://doi.org/10.1016/0306-4522(93)90029-F)
- Verkhratsky A, Shmigol A (1996) Calcium-induced calcium release in neurons. *Cell Calcium* 19(1):1–14. [https://doi.org/10.1016/s0143-4160\(96\)90009-3](https://doi.org/10.1016/s0143-4160(96)90009-3)
- Welsby PJ, Wang H, Wolfe JT, Colbran RJ, Johnson ML, Barrett PQ (2003) A mechanism for the direct regulation of T-type calcium channels by Ca^{2+} /calmodulin-dependent kinase II. *J Neurosci* 23(31):10116–10121. <https://doi.org/10.1523/JNEUROSCI.23-31-10116.2003>
- Yue B (2001) The role of H-current in regulating strength and frequency of thalamic network oscillations. *Thalamus Relat Syst* 1:95–103. [https://doi.org/10.1016/S1472-9288\(01\)00009-7](https://doi.org/10.1016/S1472-9288(01)00009-7)
- Zhang X, Min X, Xu X et al (2016) ZD7288, a selective hyperpolarization-activated cyclic nucleotide-gated channel blocker, inhibits hippocampal synaptic plasticity. *Neural Regen Res* 11:779. <https://doi.org/10.4103/1673-5374.182705>
- Zobeiri M, Chaudhary R, Datunashvili M, Heuermann RJ, Lüttjohann A, Narayanan V, Balfanz S, Meuth P, Chetkovich DM, Pape HC, Baumann A, van Luijtelaar G, Budde T (2018) Modulation of thalamocortical oscillations by TRIP8b, an auxiliary subunit for HCN channels. *Brain Struct Funct* 223:1537–1564. <https://doi.org/10.1007/s00429-017-1559-z>
- Zobeiri M, Chaudhary R, Blaich A, Rottmann M, Herrmann S, Meuth P, Bista P, Kanyshkova T, Lüttjohann A, Narayanan V, Hundedehege P, Meuth SG, Romanelli MN, Urbano FJ, Pape HC, Budde T, Ludwig A (2019) The hyperpolarization-activated HCN4 channel is important for proper maintenance of oscillatory activity in the Thalamocortical system. *Cereb Cortex* 29:2291–2304. <https://doi.org/10.1093/cercor/bhz047>

Publisher's note Springer Nature remains neutral with regard to jurisdictional claims in published maps and institutional affiliations.